UNITED NATIONS EDUCATIONAL, SCIENTIFIC AND CULTURAL ORGANIZATION
INTERNATIONAL ATOMIC ENERGY AGENCY
INTERNATIONAL CENTRE FOR THEORETICAL PHYSICS
I.C.T.P., P.O. BOX 586, 34100 TRIESTE, ITALY, CABLE: CENTRATOM TRIESTE

H4.SMR/1013-38

SCHOOL ON THE USE OF SYNCHROTRON RADIATION IN SCIENCE AND TECHNOLOGY:
"John Fuggle Memorial"

3 November - 5 December 1997

Miramare - Trieste, Italy

EXAFS Introduction

A. Fontaine
Laboratoire Louis Neel
Grenoble, France

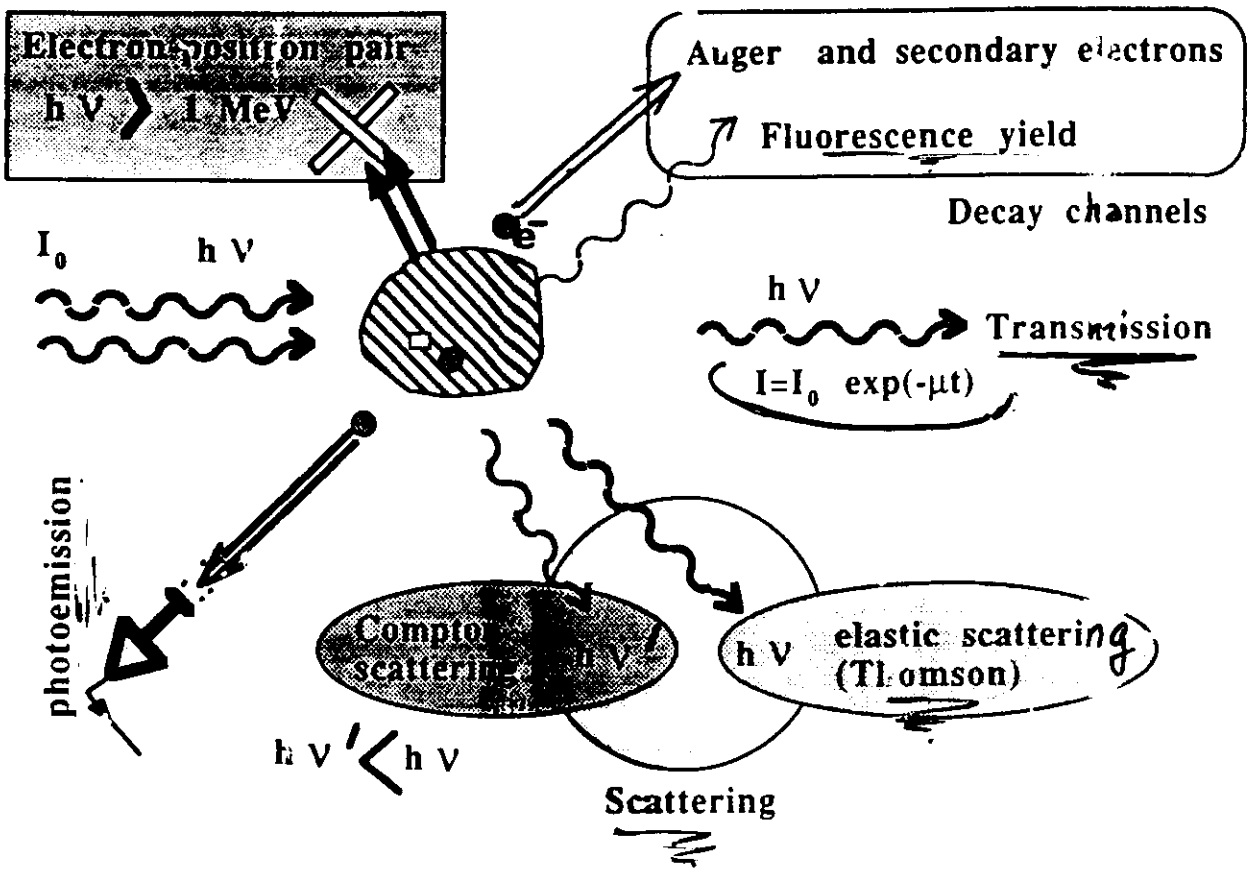

- 1 photon IN / 1 photon OUT

  Diffusion $\bar{e}$ Thomson $\left(\frac{8\pi}{3} r_e^2\right)$

- 1 photon IN / 0 photon OUT

- $\bar{e}_\gamma$ IN ABSORPTION

  $\bar{e}_\gamma$ OUT PHOTOEMISSION

$\hbar\omega$ (100 eV → 50 KeV)

INTERACTIONS with ELECTRONS ARE IMPORTANT

I.D. SECTIONS EFFICACES D'INTERACTION (Atomiques)

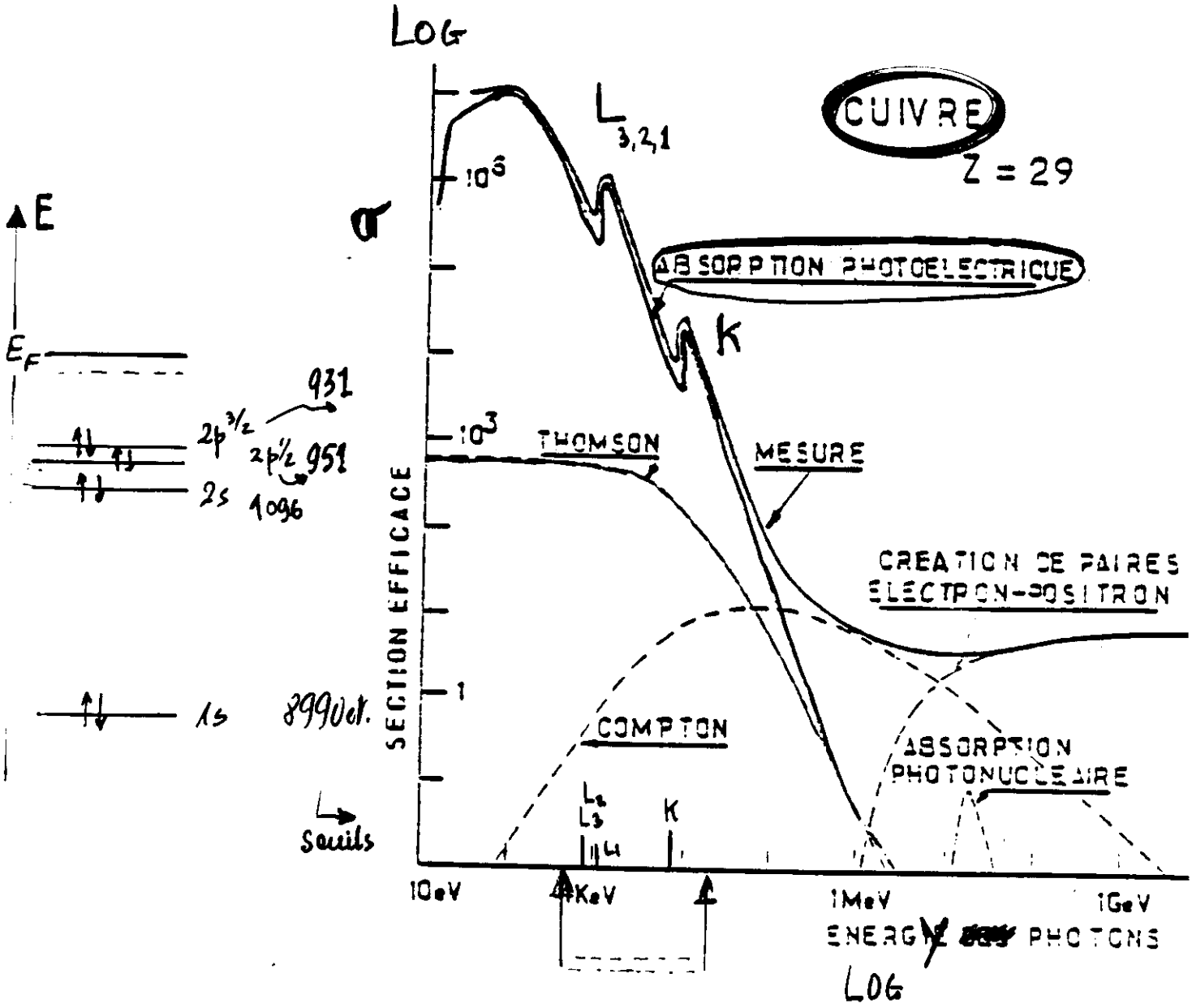

FIGURE I.5

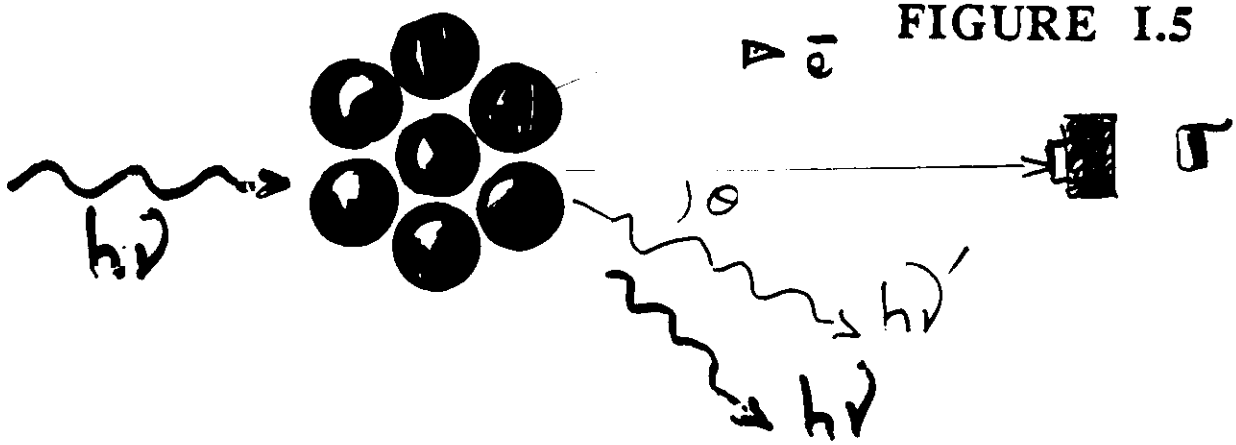

The x-ray absorption cross-section

The Golden Rule $W = e\vec{r}\cdot\vec{E}$

$$\sigma = (2\pi/\hbar)\sum_f |\langle f|W|i\rangle|^2 \delta(E_f - E_i - \hbar\omega)$$

Expansion up to the electric quadrupole term

$$\exp[i(\vec{k}\cdot\vec{r})] \simeq 1 + i\vec{k}\cdot\vec{r}$$

Absorption cross-section including electric dipole and quadrupole contributions

Dipolar

$$\sigma(\omega) = 4\pi^2\alpha\hbar\omega\{\sum_f |\langle f|\hat{\varepsilon}\cdot\vec{r}|i\rangle|^2 \delta(E_f - E_i - \hbar\omega)$$

$$+ \sum_f (1/4)|\langle f|\hat{\varepsilon}\cdot\vec{r}\,\vec{k}\cdot\vec{r}\,|i\rangle|^2 \delta(E_f - E_i - \hbar\omega)\}$$

Quadrupolar

4 TOOLS

- SELECTIVITY $\hbar\omega$ (E_i)
- DICHROISMS $\vec{\varepsilon}\cdot\vec{r}$ ($\vec{\varepsilon}\cdot\vec{z}$ or $(\varepsilon_x - i\varepsilon_y)(x+iy)$)
- SELECTION RULES dipole $\Delta\ell = \pm 1$
- FINAL STATE RELAXATION $\leq |f\rangle$

DIPOLAR SELECTION RULES

Règles de sélection dipolaires

Absorption

ℓ, s, J, m_J INITIAL
ℓ, s, J, m_J FINAL

$\Delta J = 0 \pm 1$ sauf $J=J'=0$

$\Delta \ell = \pm 1$

$\Delta m_J = 0, \pm 1$ (L) (R)

$\vec{E}$

$\Delta s = 0$

$|f\rangle = |1s^1 \ldots\ldots, np^1\rangle$

Ne

$|i\rangle = |1s^2\ 2s^2\ 2p^6\rangle$

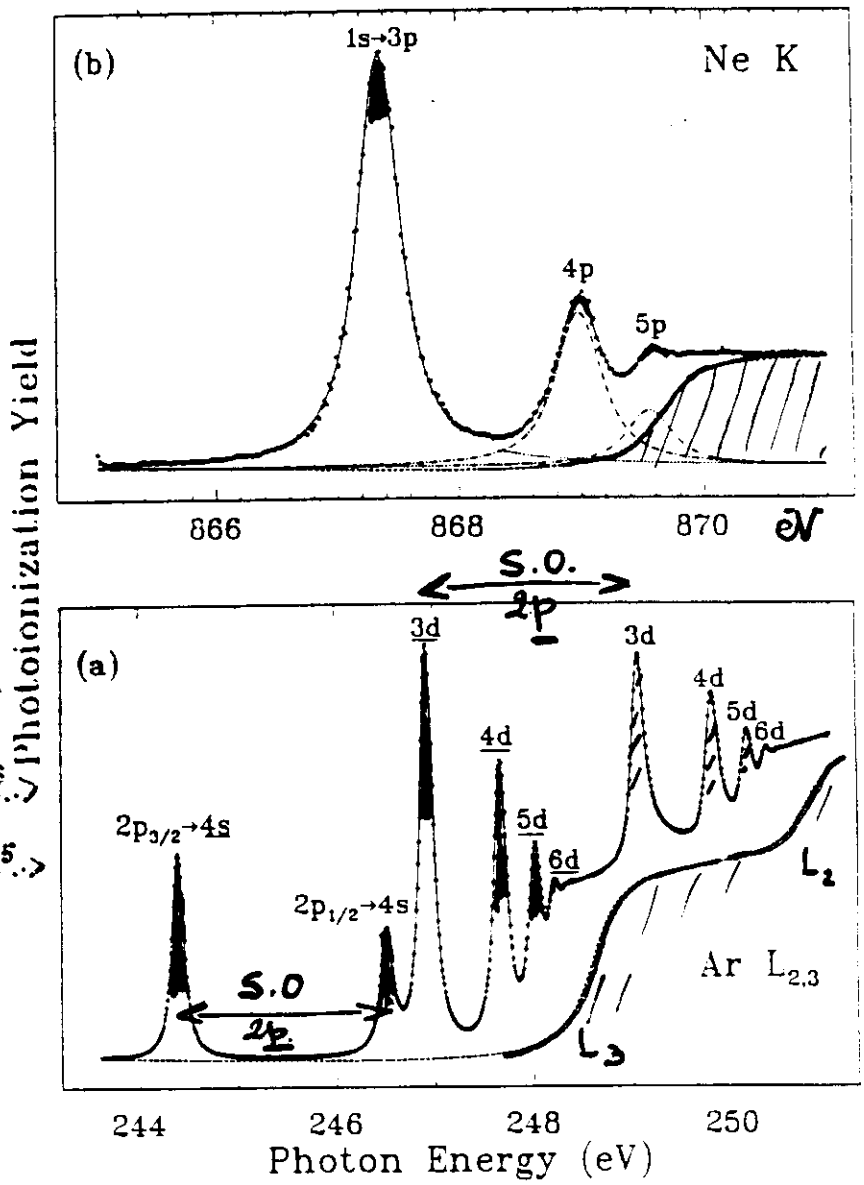

Ar

$|i\rangle = |1s^2\ 2s^2\ 2p^6\ 3s^2\ 3p^6\rangle$

$|f\rangle$ $\vec{J} = \vec{L}+\vec{S}$ $\begin{cases} \uparrow\downarrow & 1/2 \\ \uparrow\uparrow & 3/2 \end{cases} |\ldots 2p^5 \ldots\rangle$

$|f_d\rangle = |\ldots 2p^5 \ldots\ldots nd^1 \ldots\rangle \quad n \geq 3$

$|f_s\rangle = |\ldots 2p^5 \ldots\ldots ns^1 \ldots\rangle \quad n \geq 4$

Status and perspectives of high-resolution spectroscopy in the soft x-ray range (invited)

G. Kaindl, M. Domke, C. Laubschat, E. Weschke, and C. Xue

Institut für Experimentalphysik, Freie Universität Berlin, Arnimallee 14, W-1000 Berlin 33, Germany

(Presented on 18 July 1991)

Soft X. rays $\Longleftrightarrow$ Allow High energy - Resolution

MORE INFORMATIONS ACCESSIBLE

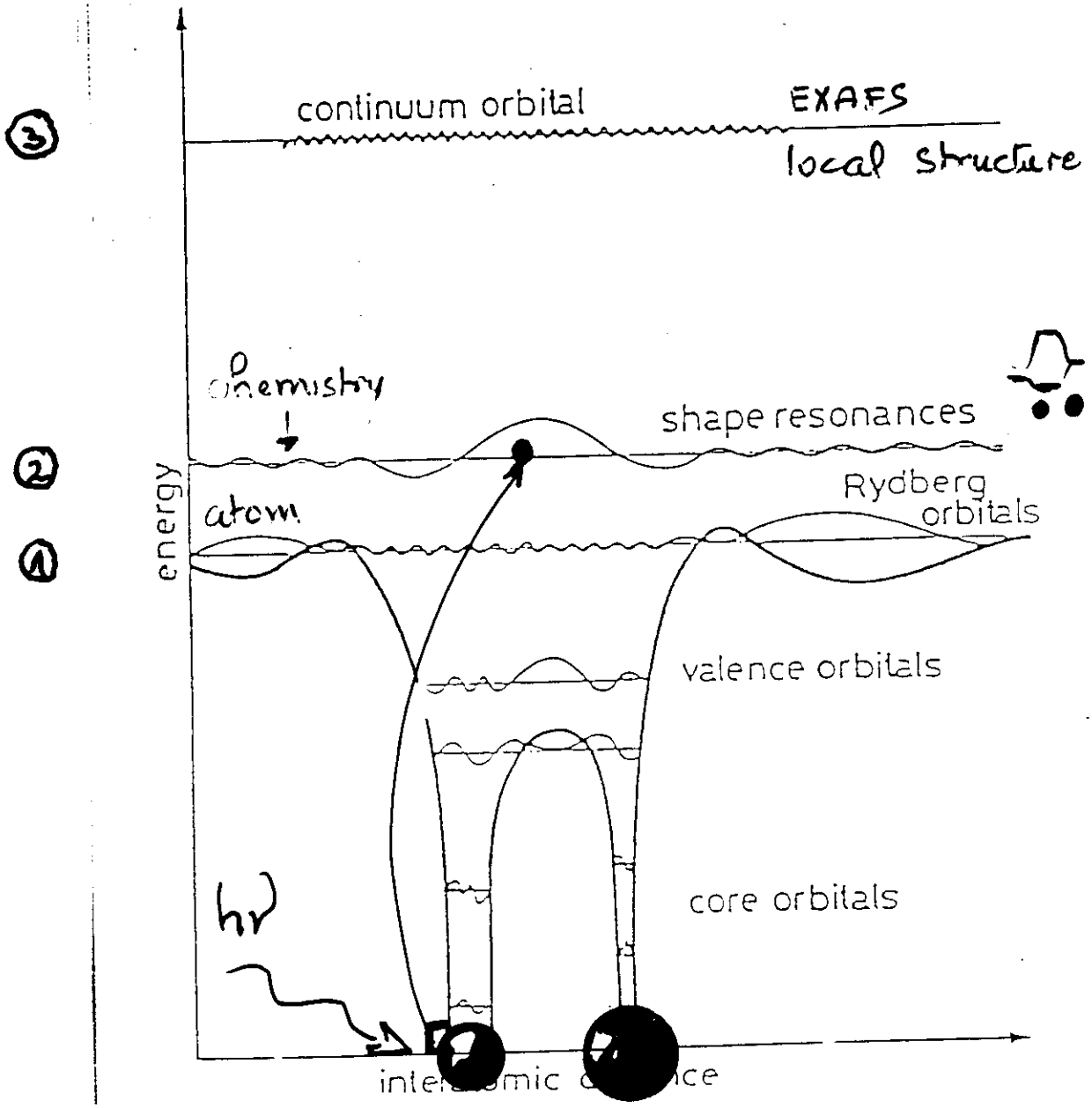

CORE HOLE in the final state

Status and perspectives of high-resolution spectroscopy in the soft x-ray range (invited)

G. Kaindl, M. Domke, C. Laubschat, E. Weschke, and C. Xue
Institut für Experimentalphysik, Freie Universität Berlin, Arnimallee 14, W-1000 Berlin 33, Germany

(Presented on 18 July 1991)

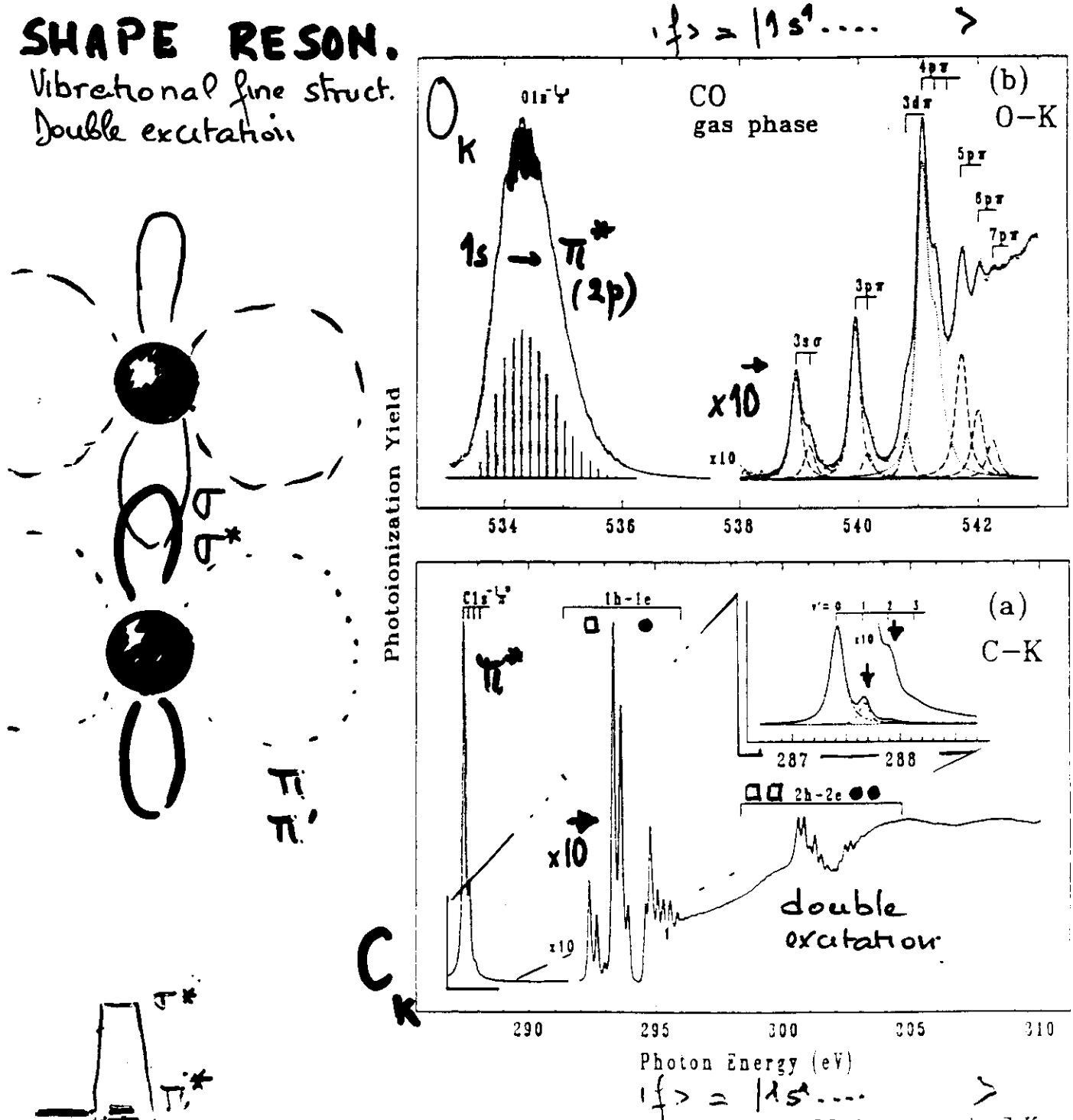

FIG. 3. Photoionization spectra of gas-phase CO close to (a) the C-*K* and (b) the O-*K* thresholds. The dominant spectral features in both spectra from excitations of C-1*s* and O-1*s* electrons, respectively, into the lowest unoccupied molecular state of Π symmetry; the resolved vibrational structure of the C $1s^{-1}\pi^*$ resonance is presented in the inset of (a). The less intense spectral features at higher photon energies (enhanced by a factor of 10 in both cases) stem from 1*s*–Rydberg-state transitions with vibrational fine structure as well as double excitations (in the C-*K* case).

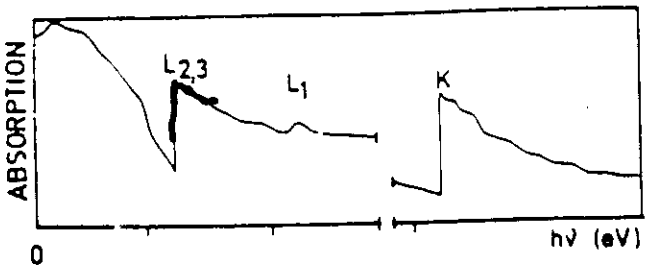

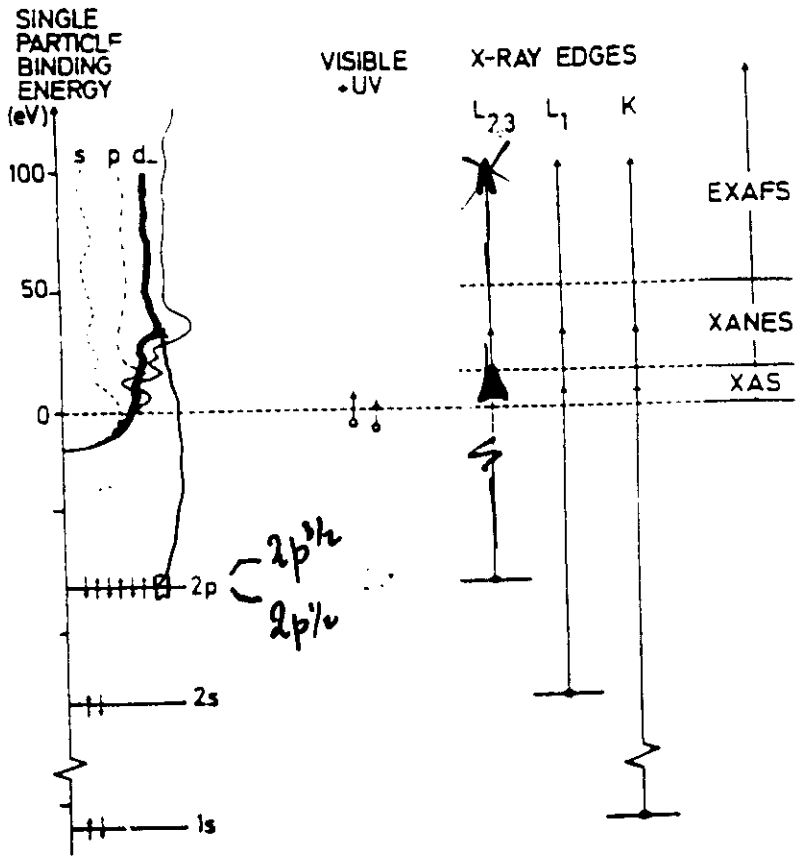

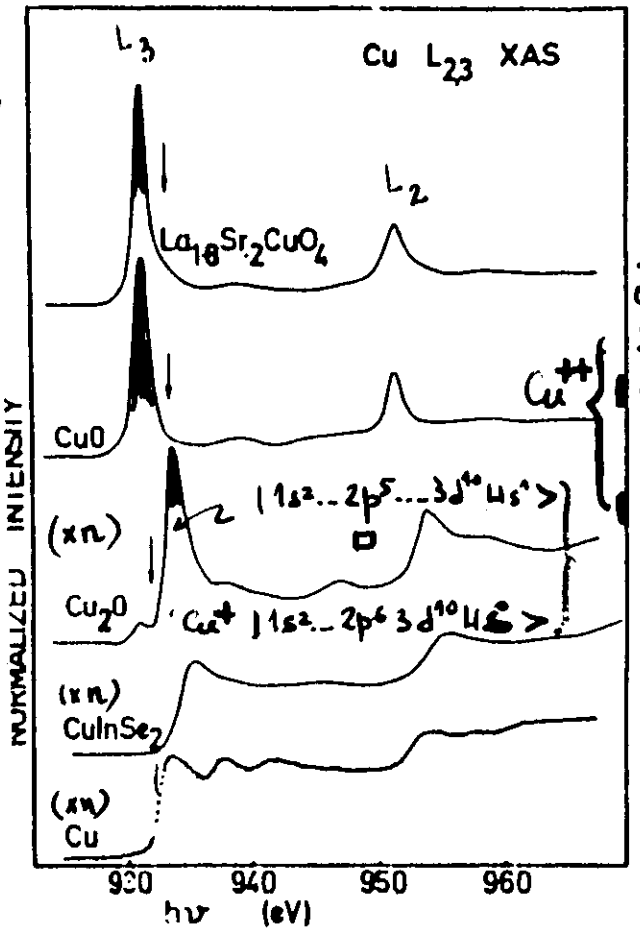

NARROW BAND

ONE-ELECTRON PICT.

INITIAL STATE

$|1s^2.2p^6.3d^9>$

FINAL STATE

$|1s^2.2p^5...3d^{10}>$

□

CORE HOLE

BROAD CONTINUUM

{ SPIN-ORBIT
{ CORE HOLE
SELECTION RULES : $\Delta l \pm 1$

KRONIG 1925

97.8 [illegible]

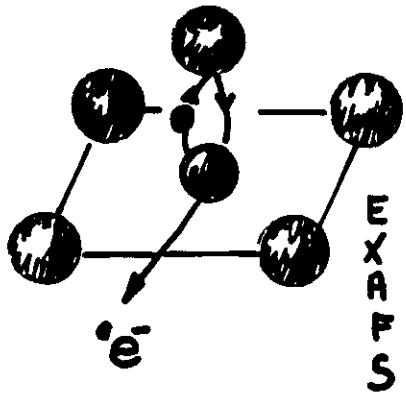

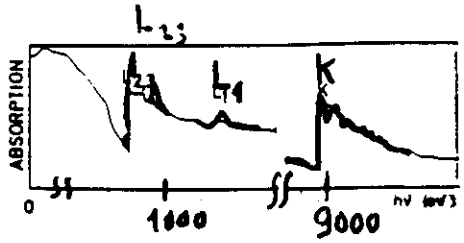

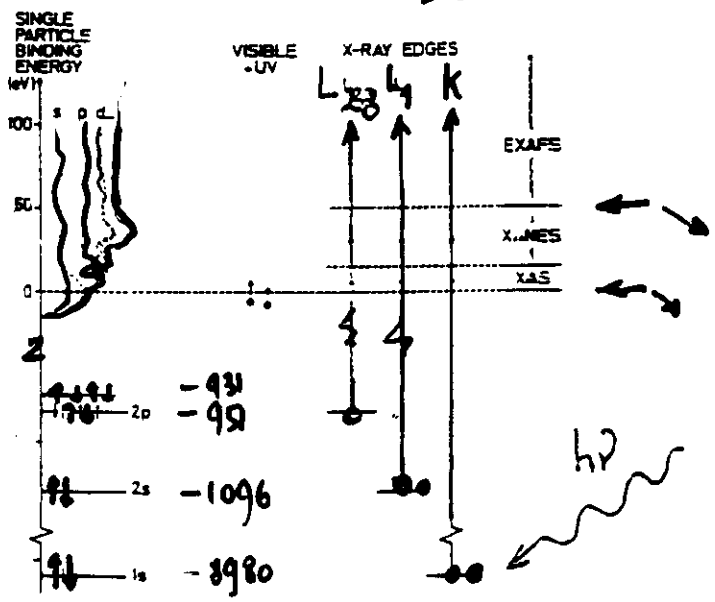

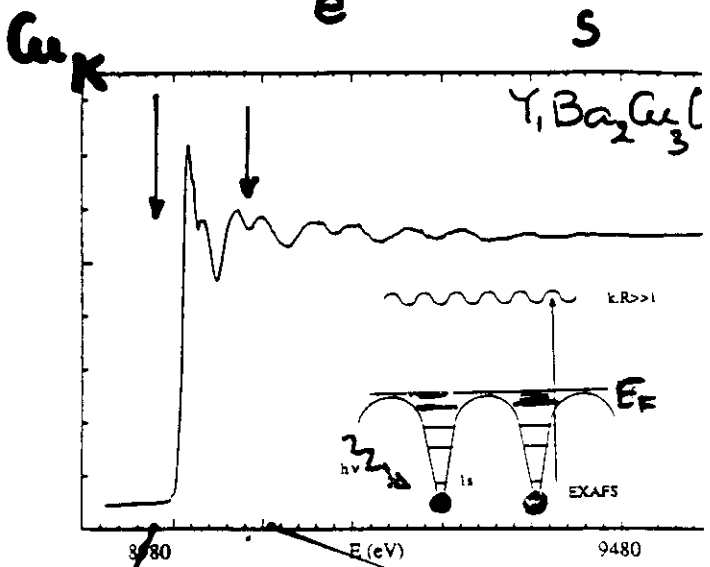

Spectre complet d'Exafs où les oscillations s'étendent au-delà de 600 eV après seuil.

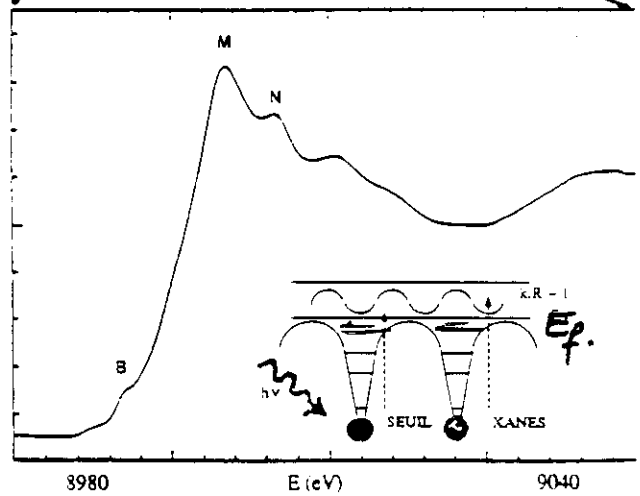

Présentation du seuil d'absorption de $Y_1Ba_2Cu_3O_{6+\xi}$ où l'on peut analyser pratiquement les transitions B, M et N propres du seuil, en termes d'orbitales moléculaires. Au delà de 20 eV on est dans le domaine du Xanes.

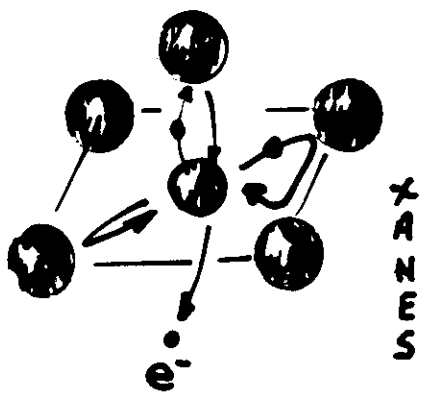

3 Séparation schématique d'un spectre d'absorption en trois zones.

XCORE HOLE . WELL SCREENED
POORLY SCREENED
* B identification of Cu^I :

SUMMARY

I. INTERACTION: DIPOL. ELECTRIC

and

II. X.A.S. Atom-selective
RDOS-selective

III POLARISATION DEPENDENT

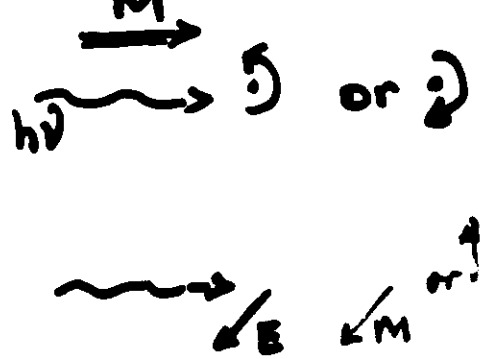

IV Multiplets $\langle f |$
or
Multiple scattering

CORE HOLE
PHOTO electron
→ FINAL STATE

or
Single scattering EXAFS
(+ε)

V SIMPLICITY of INITIAL STATE

$|i\rangle$

GROUND STATE

II EXAFS

Model : single scattering of the photoelectron

Data analysis scheme tutorials

III Data Collection

Examples. *

II.1 EXAFS & XANES : SCATTERING MODEL 97-1

EXAFS

XANES

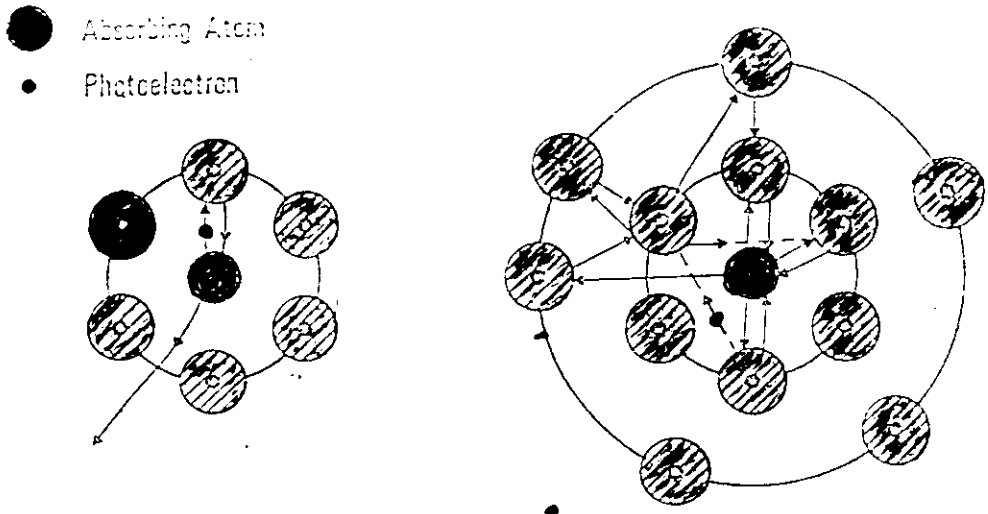

$$\mu \sim \sum_f |\langle f | \vec{R}.\vec{\varepsilon} | i \rangle|^2 \, \delta(E_f - E_i - \hbar\omega)$$

$|f\rangle = |f_0\rangle$ + (scattered wavelets)

$|f_0\rangle$: isolated atom

neighbours.

XAS : one electron picture

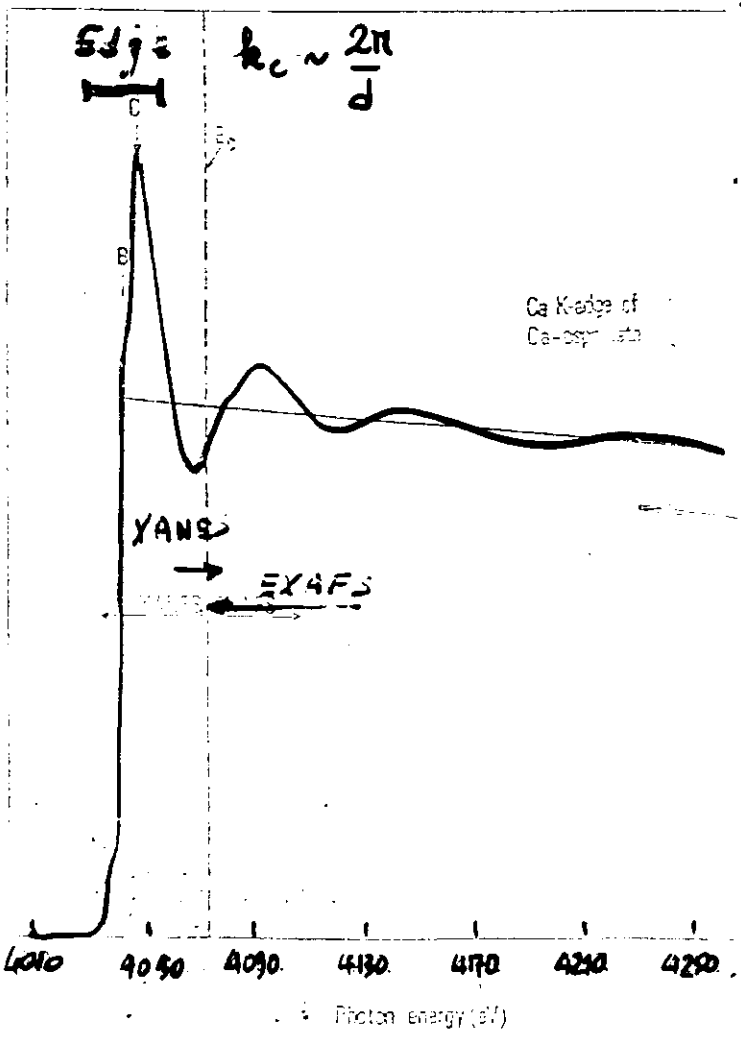

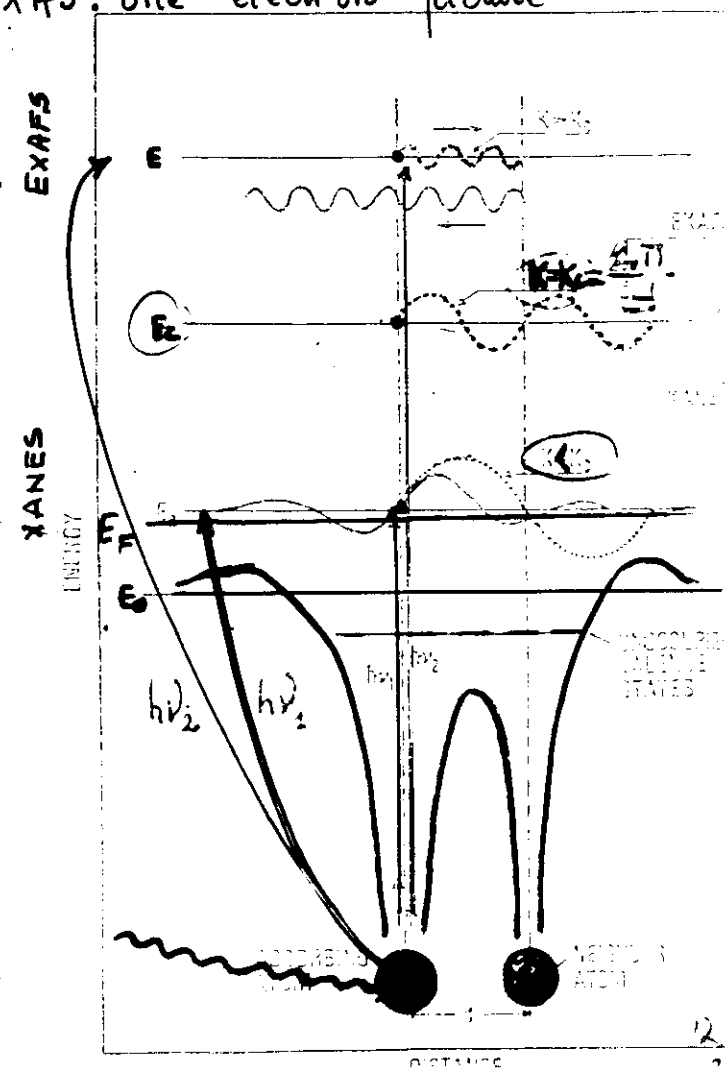

II . 1

Heuristic derivation

$$\mu = \sum_f |\langle i| \vec{R}.\hat{\varepsilon} |f\rangle|^2 \; \delta(E_f - E_i - \hbar\omega)$$

ISOLATED ATOM

ANG. RAD. PHASE.

$$Y_{l,0}\left(\frac{\vec{R}}{R}\right) h_1^l(kR)\, e^{i\delta_l'(k)}$$

$$|f_0\rangle \sim \frac{e^{i(kR_f + \delta_i')}}{2kR_f}$$

≡ OUT GOING WAVE

~ plane wave @ R_f

SURROUNDED EMITTER

$$|f\rangle = |f_0\rangle \; (1 + \chi)$$

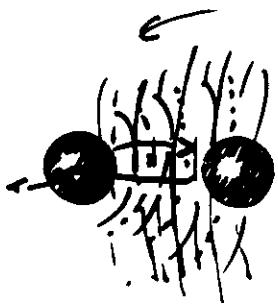

Backscattering

$$f_f(\pi, k) = \frac{1}{2ik} \sum_l (2l+1)(e^{2i\delta_l} - 1) P_l(-1)$$

coming back on the central atom

$$\frac{e^{ikR_f}}{R_f} \; e^{i\delta_i(k)}$$

EXAFS SIGNAL for a SINGLE BACKSCATTERER

$$\chi(k) = \frac{\mu - \mu_0}{\mu_0} = \frac{-|f_f(\pi,k)|}{kR_f R_f} \sin\left(2kR_f + [2\delta_i' + \Phi_f]\right)$$

- $\chi(k) = \dfrac{\mu - \mu_0}{\mu_0}$

- $\chi(k) = -\dfrac{1}{k} \sum_j \dfrac{1}{R_j^2} \left| f_j(\pi, k) \right| \sin\left(2k R_j + 2\delta_1(k) + \theta\right)$

Powder or cubic lattice $\sum N_j$ j^{th} shell $\times e^{-2\sigma_j^2 k^2} \cdot e^{-\frac{R_j}{\lambda}}$

. $\dfrac{\hbar^2 k^2}{2m} = E - E_0$ origin of the kinetic energy

. $e^{-\frac{R_j}{\lambda}}$ mean free path of the photoelectron

. $e^{-2\sigma_j^2 k^2}$ D.W. static or dynamic disorder

ADVANTAGES of EXAFS.

(I) SELECTIVITY of the "ELECTRON" SOURCE

Cu K 8979.8 Zn K 9659 Eu L_{III} 6977 eV.

(II) GOOD ACCURACY IN BOND LENGTH DET
0.01 Å

(III) CHEMICAL IDENTIFICATION of NEIGHBORS
& COORDINATION NUMBER

ΔZ large enough / $\pm 1/4$ in best cases (OUT of 12)

NEEDS

PHASE SHIFTS
& BACKSCATTERING AMPLITUDES

$$\text{MAX} \leftarrow 2kR + \phi \simeq \frac{\pi}{2} + n\pi$$

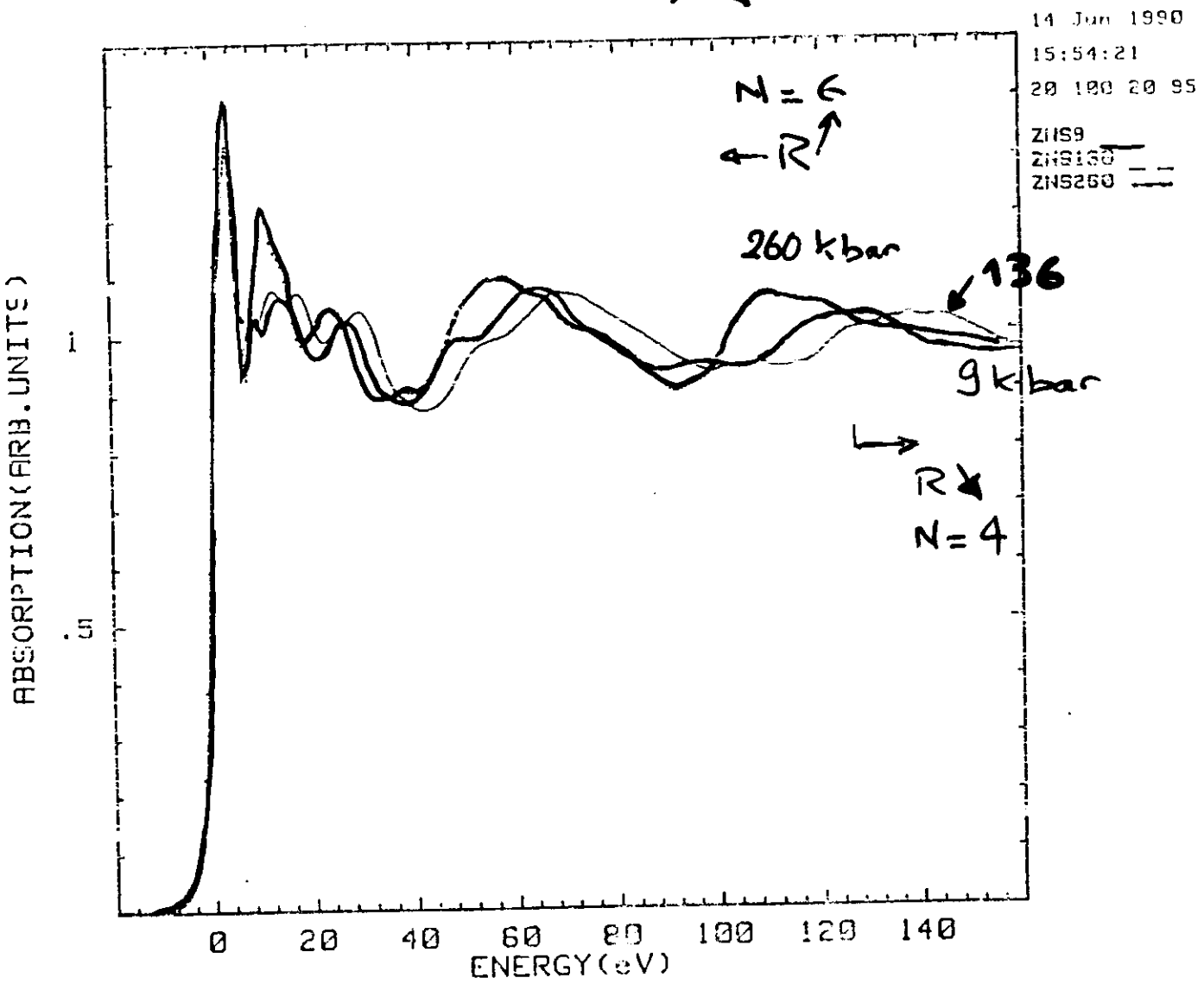

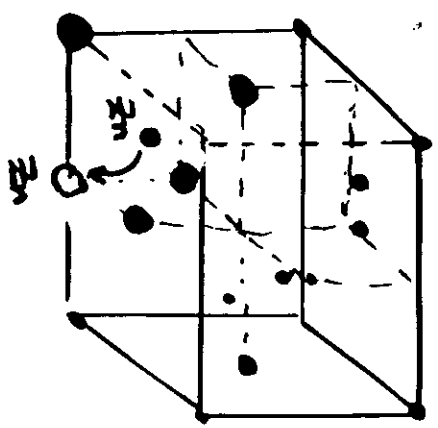

zinc blende (4

Zn.S Zn K-edge.

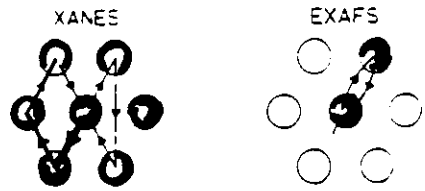

Mn dans des sites octaédrique et tétraédrique

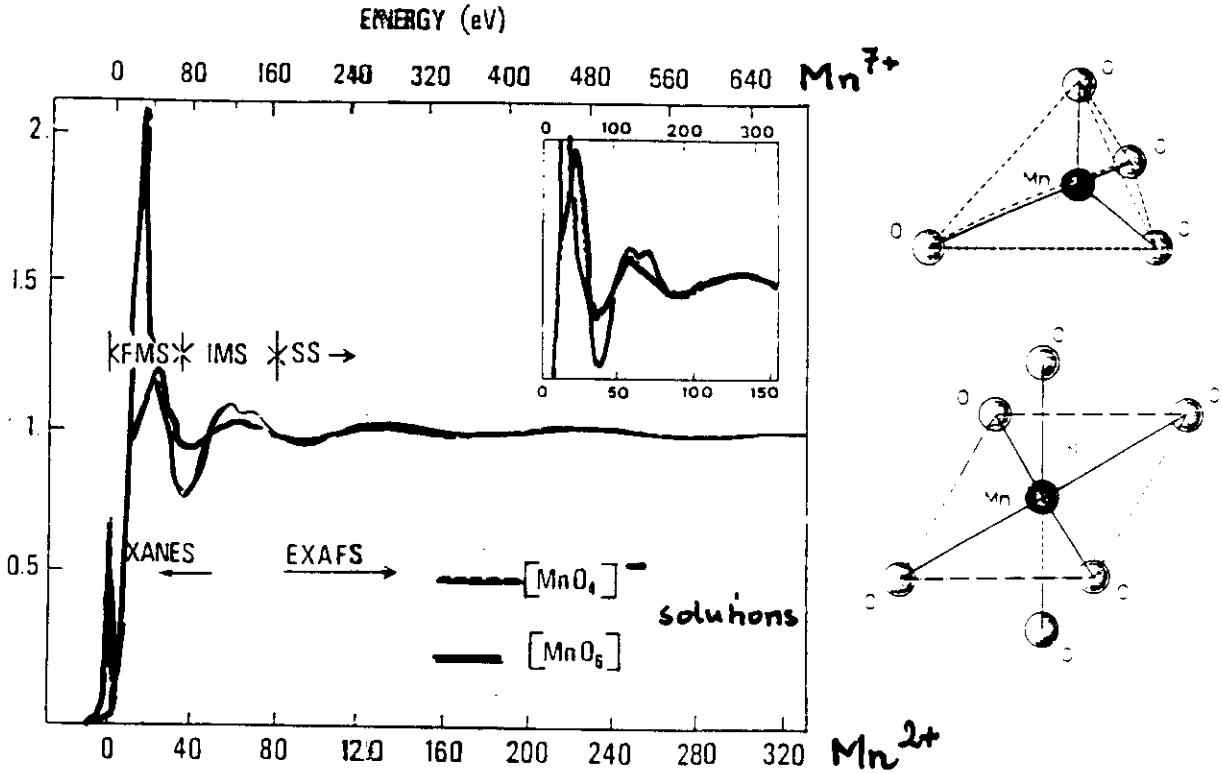

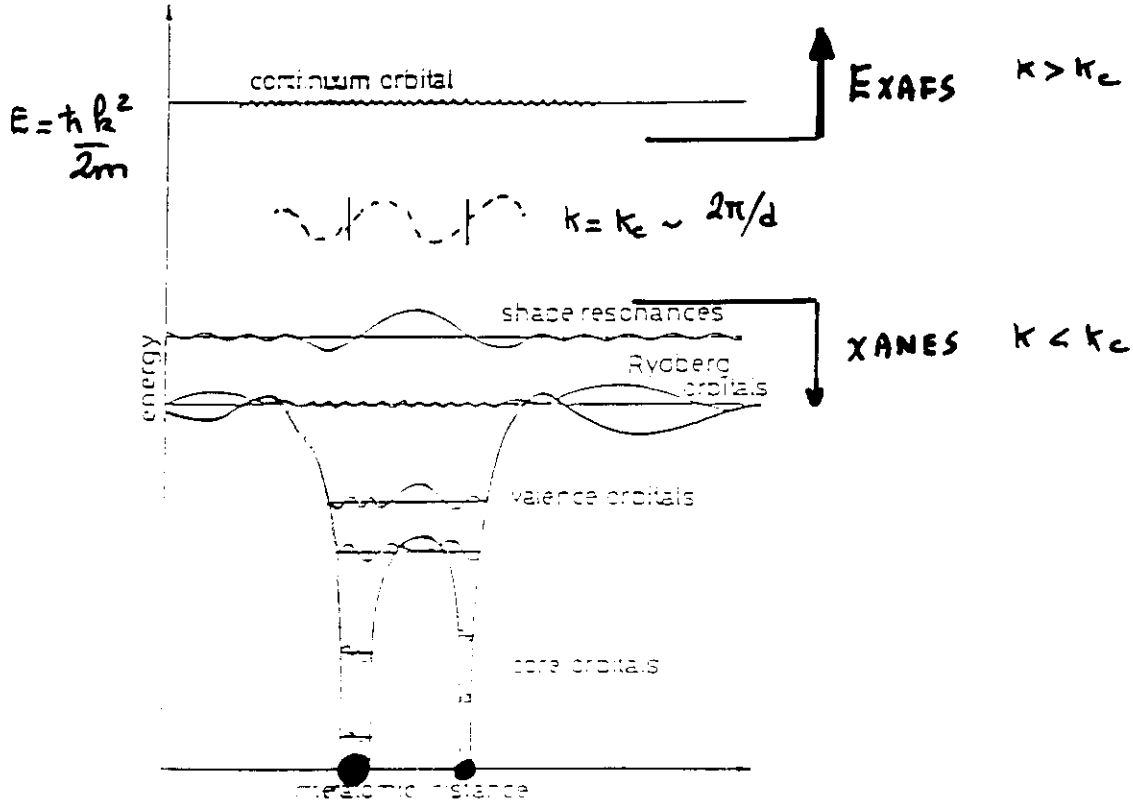

III . 4

SUMMARY

EXAFS ≃ SPHERICAL LEED

≃ DIFFRACTON OF LOW ENERGY ELECTRON

where the SOURCE OF $\bar{e}$ is
INSIDE THE SAMPLE
ON A SELECTED ATOM

EXAFS and OTHER SCATTERING TECHNIQUES

◆ X. RAY SCATT. PAIR CORRELATION . FUNCT.
Binary alloy AA
AB
BB

Bad News EXAFS does not see long distances

Good News EXAFS is accurate to evaluate local ORDER

◆ NEUTRONS $b > 0$ $b < 0$
GOOD CONTRAST

EXAFS $f_t(\pi, k)$ & its PHASE

◆ X. Ray . WEAKER INTERACTION THAN $\bar{e}$
STRONGER —— THAN $\bar{e}$

Hard X-rays Sample "REASONABLE VOLUME"

III.3 c

DEBYE . WALLER DAMPING

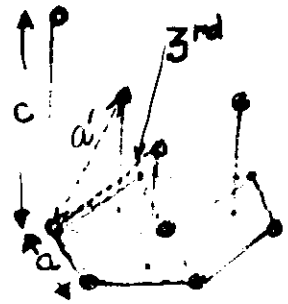

$a' = 2.912$ Å $a = 2.66$ Å

$c/a = 1.86$

$r_3 = 3.925$ Å at 25 K.

Crystallographic data.

Zn : 25 K

Zn : 300 K

Désordre thermique croit avec le n° couche

Refs etal. : Ge, Cu Analyse avec $\theta_{Einstein}$

III.3.b

Mean free path of the photoē

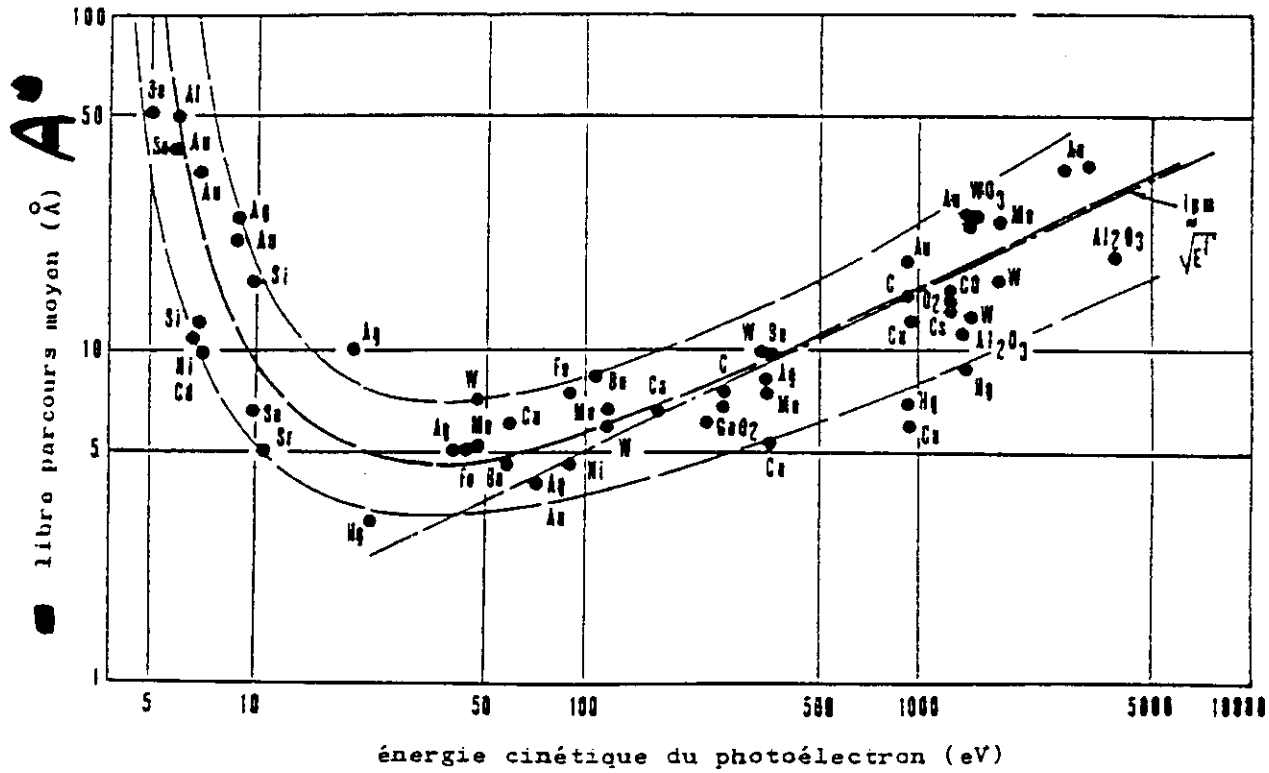

→ eV

$\lambda \propto \frac{1}{E_c}$

$E_{K.E} > 50$ eV

Figure I.6 - d'après C.R. Brundle (référence / 3 /).
Libre parcours moyen des électrons dans un solide en fonction de leur énergie cinétique.

"universal" ?

$\lambda \sim k$ a.u.

JJ.

$$\chi(k) = -\frac{[\text{illegible}]}{kR_j^2} \sin(2kR_j + \phi)\ 3\cos^2\theta_j$$

$$\cos\theta_j = (\vec{E}, \vec{R_j})$$

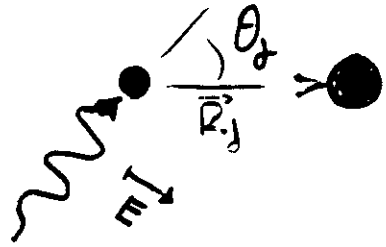

AVERAGING $\longrightarrow \langle 3\cos^2\theta_j \rangle = 1$

ASSUMPTIONS

- 1 $\bar{e}$ transition
  + INGREDIENT (corehole relaxation)
- Plane wave
- SINGLE SCATTERING

} NOT NECESSARY USED for
1/ SAKE OF CLARITY
2/ PRACTICAL APP.

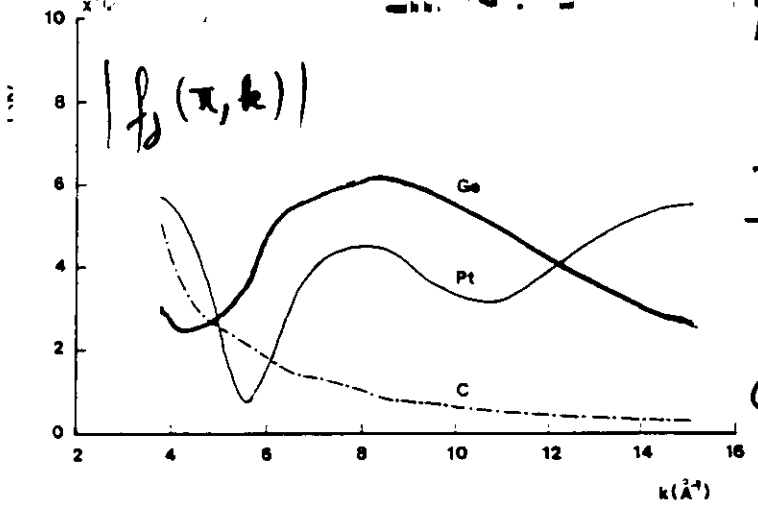

Figure 6.4. Theoretical backscattering amplitudes versus k for C ($Z = 6$), Ge ($Z = 32$), and Pt ($Z = 78$) after Teo and Lee (14).

Σ amplitudes

Pt

Ge

C

Total phase

$2kR_j + \Phi(k)$

$\Phi(k) = 2\delta_1(k) + \theta_j(k)$

- $\left\langle \frac{1}{2}\frac{d(\Phi(k))}{dk} \right\rangle \lesssim 0.40$

low Z elements

high Z: $\Phi(k)$ non monotoneous.

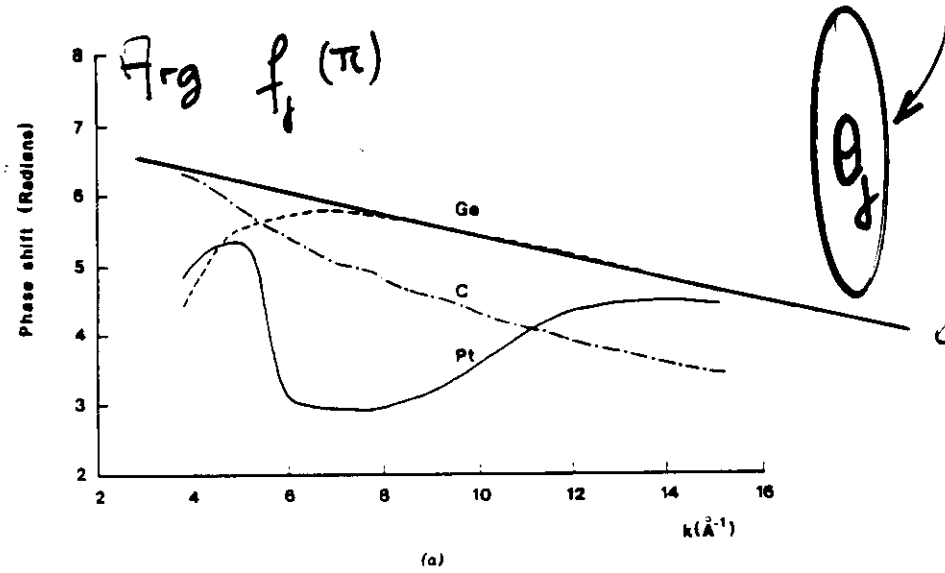

θ_j

average slope

-0.15 Å

$\frac{d\theta_j}{d(2k)} \sim 0.05$ Å

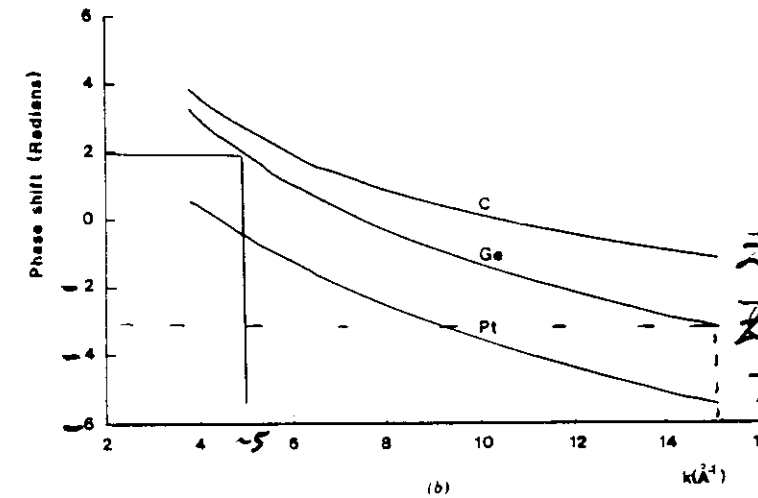

$Z = 6$ C

$Z = 32$ Ge

$Z = 78$ Pt

$2\delta_1$

$\left\langle \frac{1}{2}\frac{d(2\delta_1)}{2dk} \right\rangle = -\frac{0.5}{2}$ Å

Figure 6.5. (*a*) Theoretical scattering phase shifts for carbon, germanium, and platinum versus k. (*b*) Theoretical central atom phase shifts for carbon, germanium, and platinum. All calculations are from Teo and Lee (14).

Phase $= 2kR_j + 2\delta_1(k) + \Theta(k)$ $\Rightarrow$ VERY GOOD EVALUATION of DISTANCES

85% 13% 2%

III 5.2 Phase shifts & amplitudes

* Theoretical evaluations

  Excellent for phase shifts

  GOOD for AMPLITUDES

* Best procedure to evaluate $f(\pi)$ for the AB pair

  a/ Measure a well-known sample
  with a simple lattice
  with a structure close to the
  UNKNOWN sample
  with **A** as absorber
  B as backscatterer

  b/ Extract phase shift $+(k)$
  and amplitudes $|f(\pi), R|$

  c/ Transfer into the data analysis
  of the unknown sample.

* KEEP STANDARDS & INVESTIGATED SAMPLES
  AS CHEMICALLY CLOSE AS POSSIBLE

* WELL-CONDITIONNED PROBLEM
  HIGH PRESSURE EXP. SAMPLE @ $P=0$ ⇒ STANDARD

III. 4 EXAFS: LOCAL & SELECTIVE PROBES

useful for

- isolated IMPURITY in a MATRIX.
  local distorsion
- local symmetry determination.
  tetra or octahed. sites
- small particles
  Clusters (metallization), catalysis
- dilute samples

SURFACE PHYSICS	< monolayer on SURFACE (EXAFS
PHYSICS	Phase transformation Actual phase of sandwiched [illegible] Thin films ... , Sup a
BIO PHYSICS	Fe in Hemoglobin. Reactivity CO, O_2
GEOPHYSICS	High Pressure, High Temp.
CHEMISTRY	In-situ experiments Battery, Electrochemist
MATERIALS SCIENCE	Sup a conductors Semiconductors Insulators Magnetic alloys ...

II-2 DATA ANALYSIS

a/ SCHEME

$$\begin{cases} \Delta E_0 = E_0 - E_{threshold} \\ \dfrac{\hbar^2 k^2}{2m} = E - E_0 \end{cases}$$

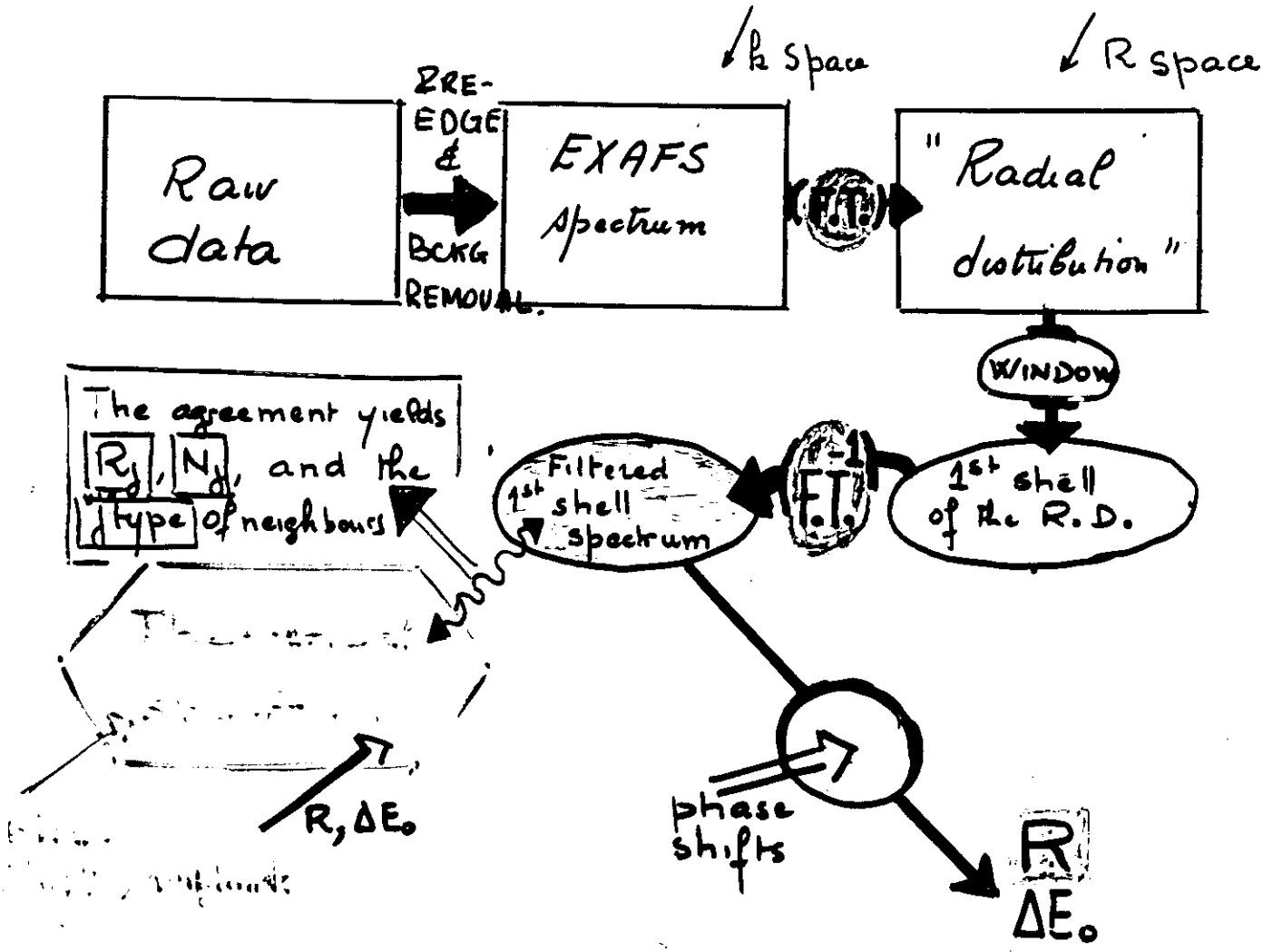

HOMOGENEOUS SHELL

fitting

O/Rh 23.2keV ~/ SAYERS · 2/ 11k /-3/ extended over 300 eV 23, 2 KeV SSRL 4/1 c.c. Stra

RH FOIL NT LONG SCAN 3/63 1005 8 8 2-22-81

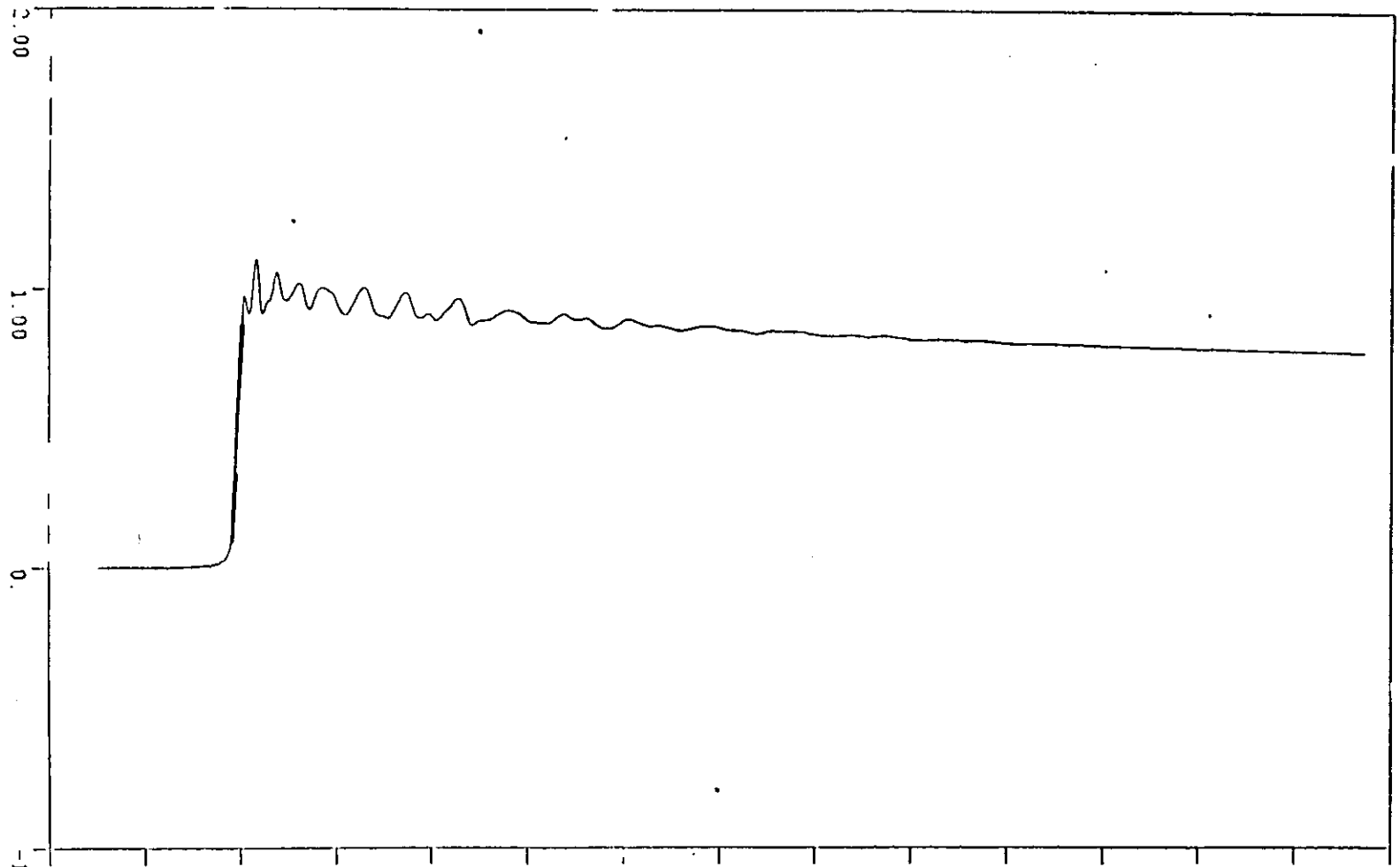

77K.

PBK PTS: 1- 12 GLITCHS: 0- 0: 0- 0: 0- 0: 0- 0: 0- 0: 0-

0: 0- 0: 0- 0: 0- 0: 0- 0: EO= 0.0

R4

3264 eV.

I.S.E. Rh foil & evaluation of accuracy in R, N determinations in the best conditions for both experiment & data handling

III.5.d

EXAFS SIGNAL

17 oscillations
⇒ Accuracy limited by phase shifts knowledge

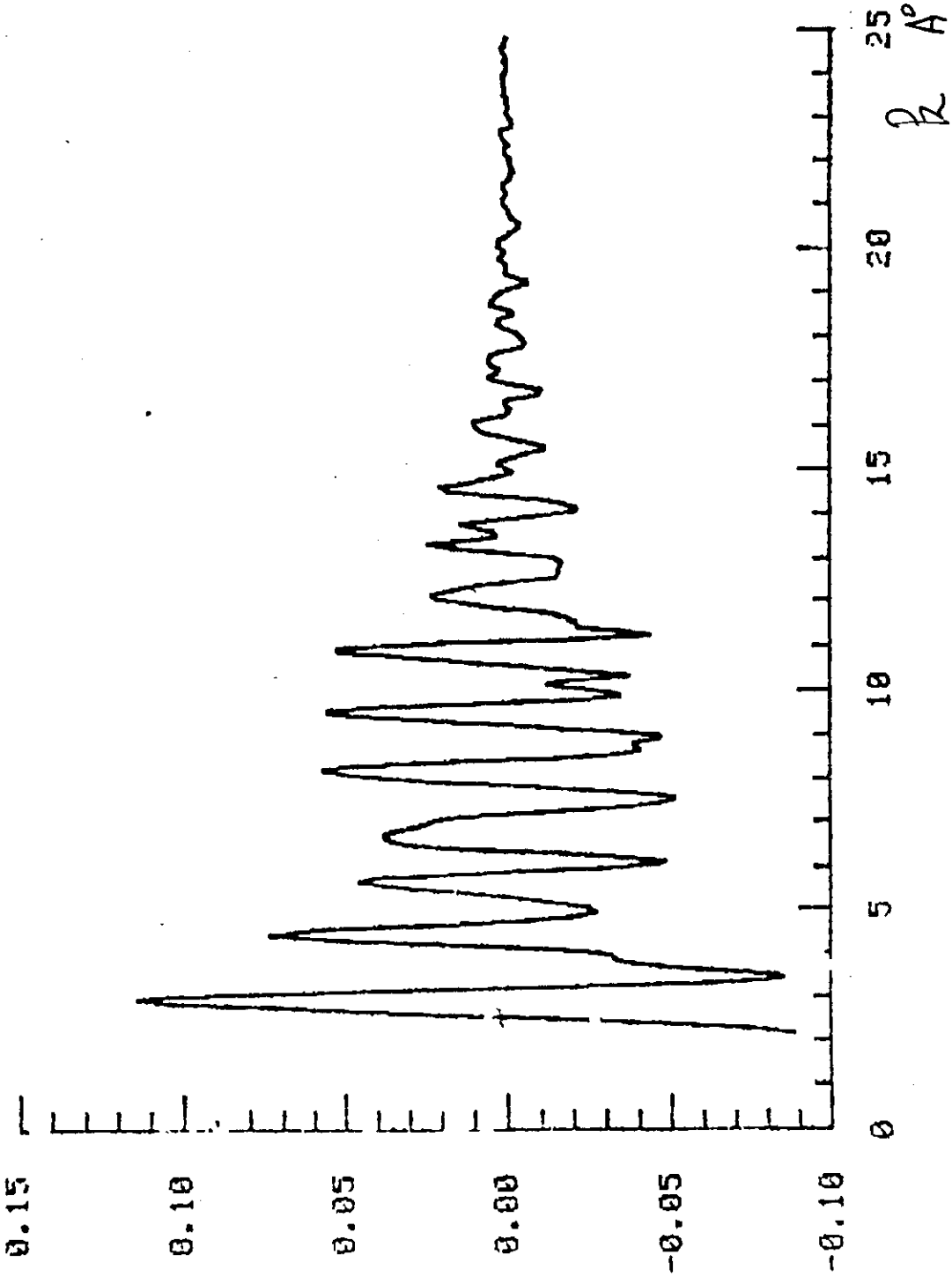

$k^3 \chi(k)$.

RH FOIL NT LONG SCAN 3/63 1005 F.T. 8 8 2-22-81

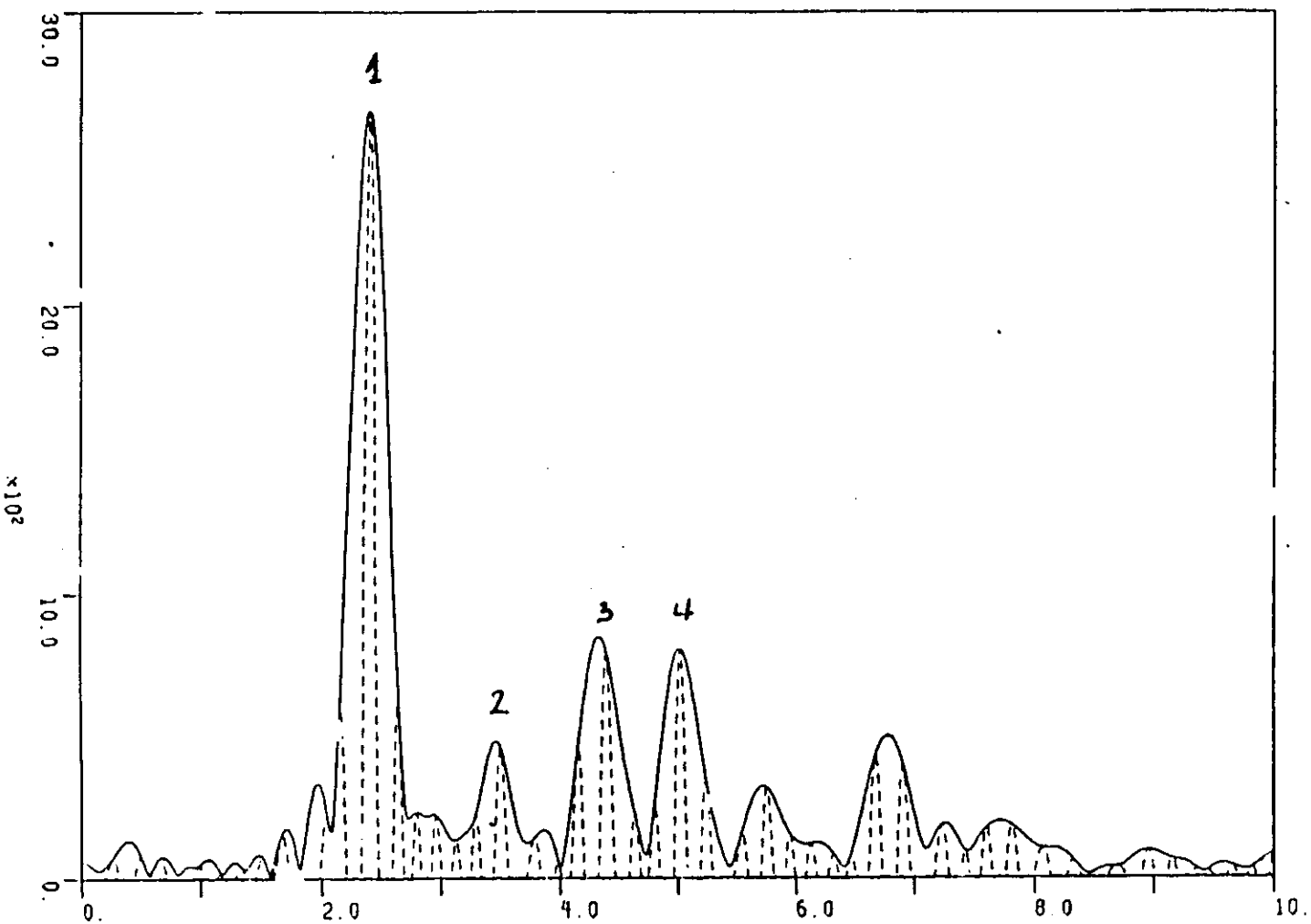

PBK PTS: 1- 12 GLTCHS: 0- 0: 0- 0: 0- 0: 0- 0: 0- 0: 0-

0: 0- 0: 0- 0: 0- 0: 0- 0: EG= 0.0 CBK PTS: 74- 399 SM=0.

2620 WE=1 0000 SEG= 0 WT=3.00 FH=.0 TR: 2.60-18.40 RM=10.00 DR=.010

Rhodium Foil. (-fc) (Data SSRL)

D. SAYERS. NCSU. line I 5 Feb 81.

shell #	k-range	λ	N	R	$\Delta\sigma^2 \times 10^4$ Å^2	E_0(eV)
MODEL → 1	5 - 17	λ_1	12	2.69	2.23	-.24
1	6 - 16	"	11.8	2.69	2.13	.42
2	5 - 17	"	4.77	3.80	1.96	-.06
2	6 - 16	"	4.78	3.80	1.97	-.24
3	5 - 17	"	24.7	4.67	3.12	-.4
3	6 - 16	"	25.1	4.67	3.21	-.4
4	5 - 17	"	12.1	5.38	3.14	+.4
4	6 - 16	"	12.78	5.38	3.38	+.2

A^{0-1}

Phase shift & Amplitude

EXAFS ANALYSIS

Not "TOTALLY" SOLVED ?

- Phase shifts and Amplitude TRANSFERABILITY
  App. Muffin Tin
- Many body problems

BREAKTHROUGH

- MULTIPLE SCATTERING

C. Natoli
P. Durham
J. Rehr
(FEFF code)

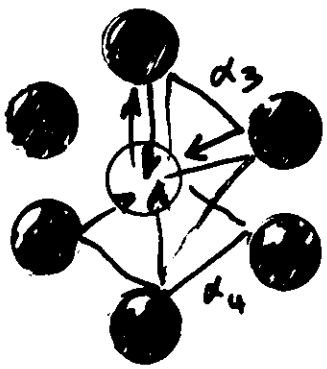

Long "multiple" paths
- Less efficient
- more numerous

- CUMULANT ANALYSIS σ^2, c^3 (T)

C. Dagg, L. Träger, D. Arvanitis, K. Baberschke J. App Phys (1993)

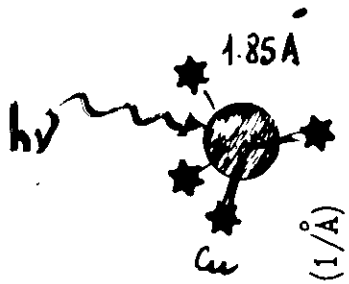

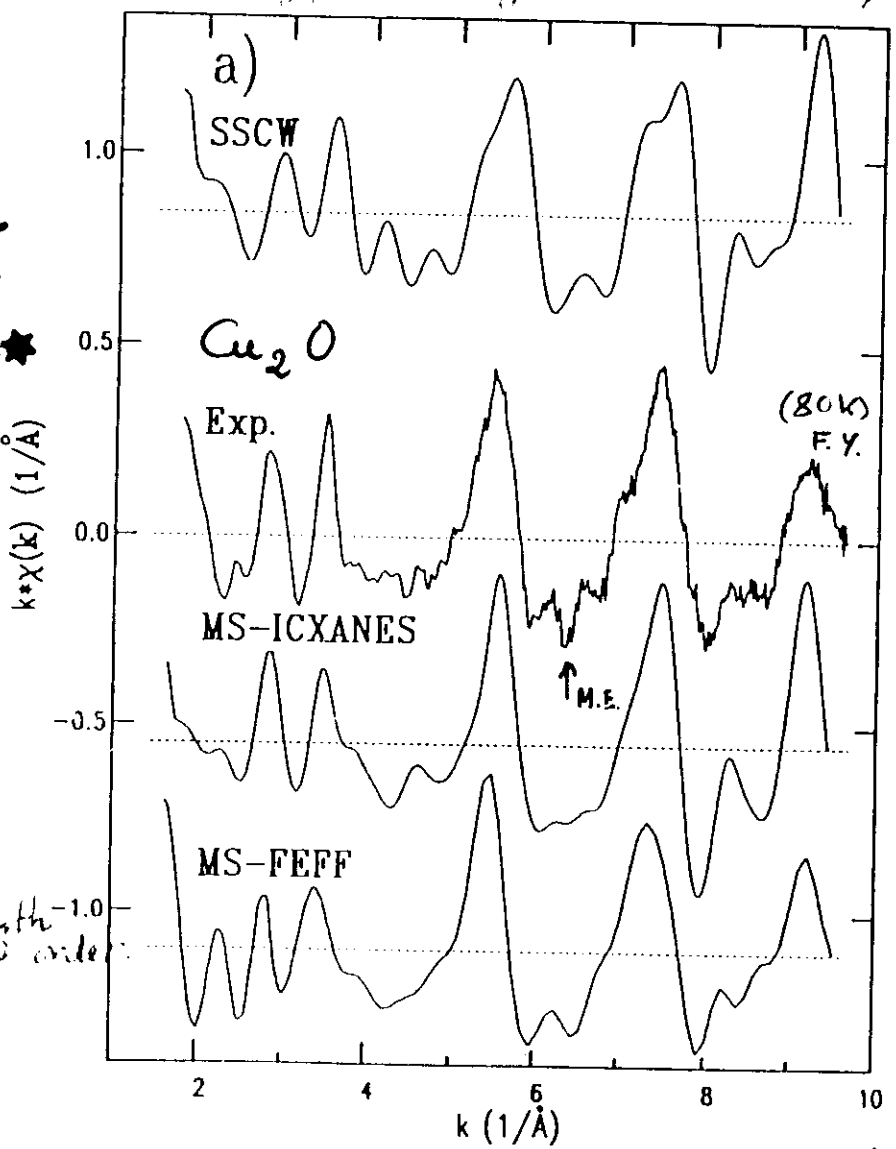

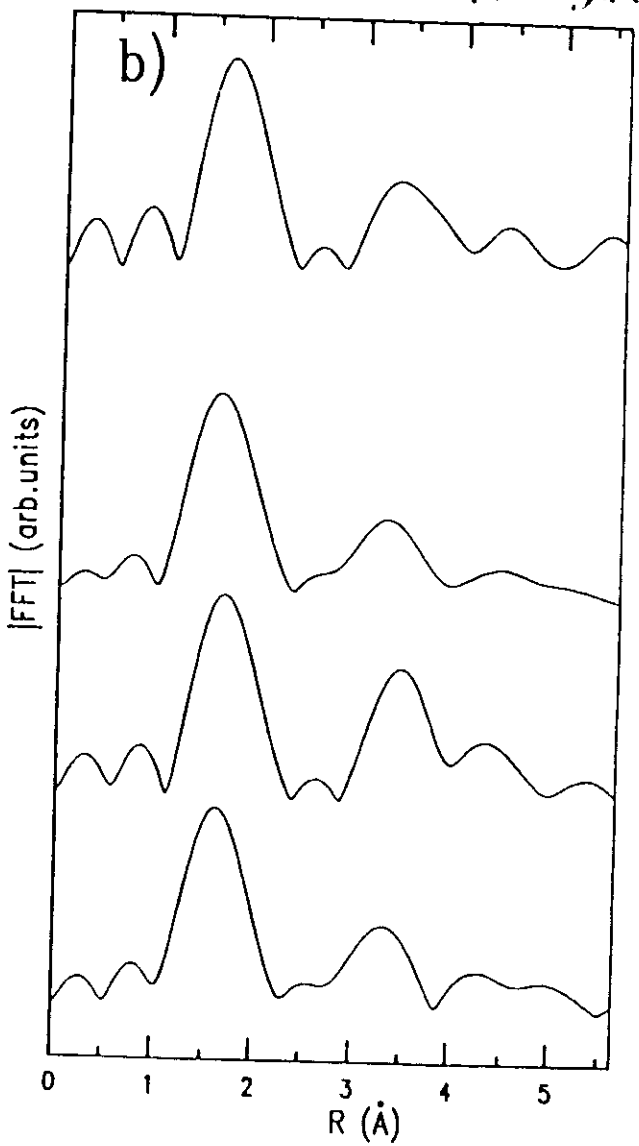

Oxygen K-edge

~ 3110 eV

Fig. 3

97.30

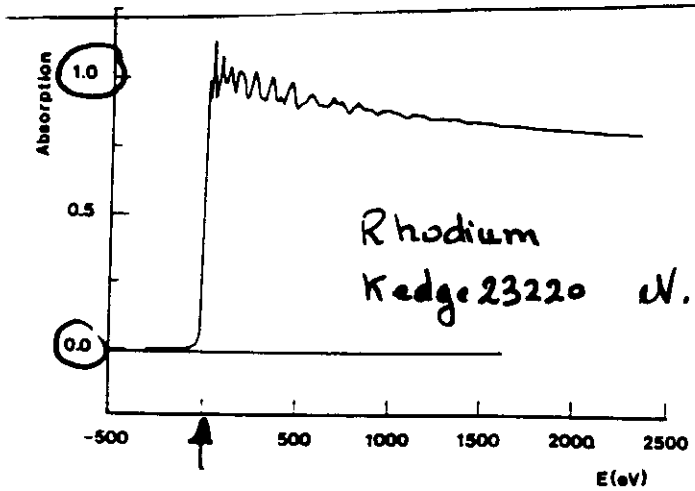

(c)

1 PRE. EDGE REMOVAL
2 + NORMALISATION

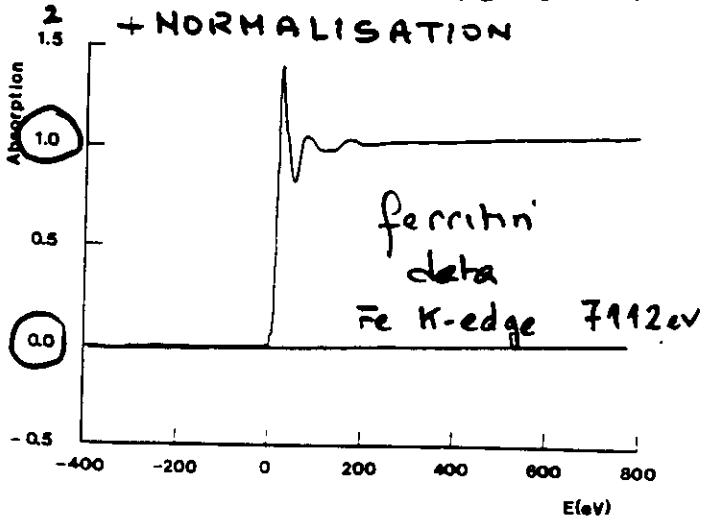

(d)

Figure 6.1. (*Continued*)

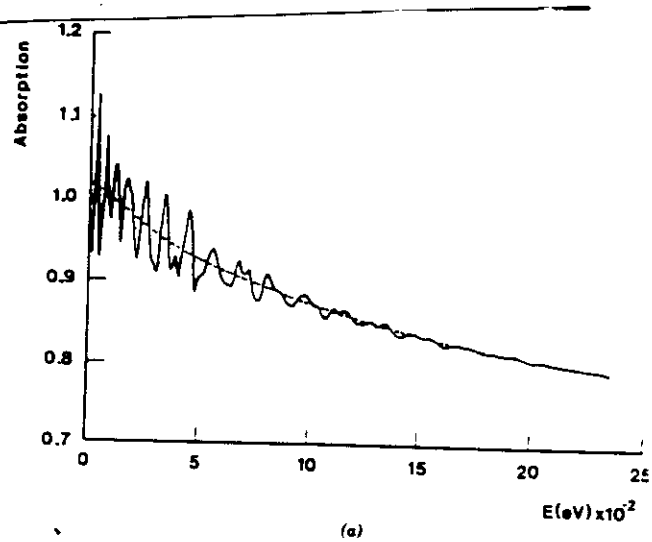

(a)

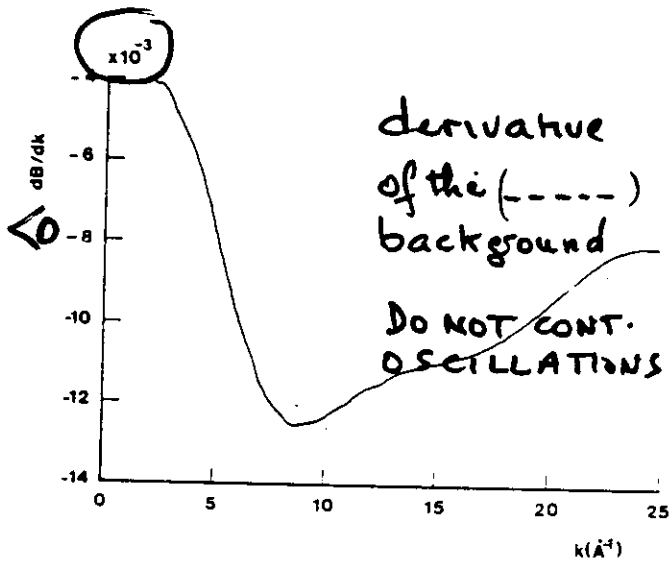

(b)

Figure 6.2. (*a*) The normalized data of Fig. 6.1*c* for rhodium metal showing on an expanded sc for the data above the edge. The calculated background curve used to extract the EXAFS is sho as a dashed line. (*b*) The derivative of this background curve versus the photoelectron wave vec *k*. (*c*) The normalized EXAFS for rhodium metal plotted versus *k*.

3 Choice of E_0 as the inflection point.

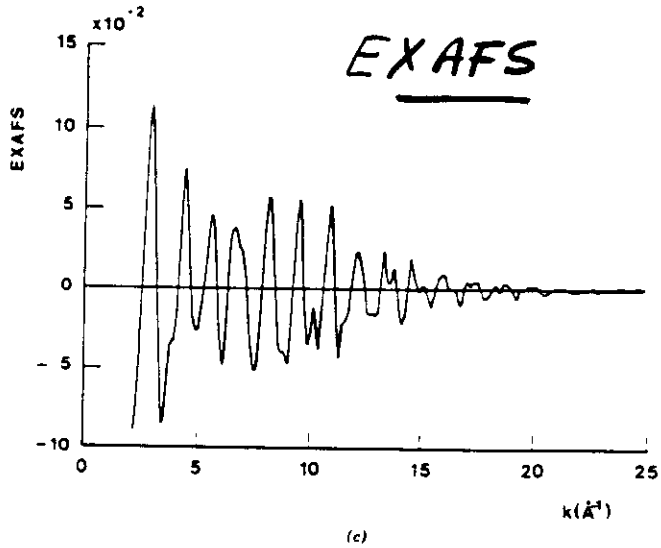

(c)

Figure 6.2. (*Continued*)

D. SAYERS, B. A. BUNKER
Ch 6. EL Koningsberger, Zinz
J. Wiley. Chemical Analysis 92

V CONCLUSIONS

What do we (try to) learn ?

1. FERMI GOLDEN RULE + DIPOLE APPROXIMATION

$$\mu \propto \sum_f |\langle f | \vec{\varepsilon}\cdot\vec{r} | i \rangle|^2 \; \delta(E_f - E_i - \hbar\omega)$$

- $|i\rangle$ site selectivity
- $|f\rangle$ DOS selectivity
  + selection rules
- $\vec{\varepsilon}\cdot\vec{r}$ Anisotropy sensitivity & any sym. breaking
- $|f\rangle$ CORE-HOLE RELAXATION VALENCE SENSITIVITY

2. EXAFS

$$\chi(k) = -\frac{1}{k} \sum_j \frac{N_j}{R_j^2} 3\cos^2\theta_j \exp(-2\sigma_j^2 k^2) \exp(-2R_j/\lambda(k))$$

$$|f_j(\pi,k)|$$

$$\sin(2kR_j + 2\delta(k) + \arg f_j(\pi,k))$$

- Anisotropy sensitivity
- "SPHERICAL LEED" (Low Energy Electron Diff)
- Sensitivity to disorder.

EXAFS = STRUCTURAL PROBE with LOCAL ABILITY, ie for COORDINANCE

COMPLEX BACKSCATTERING AMPLITUDE
PHASE + AMPLITUDE

WHAT don't we learn ?

details
+

- XANES (multiple scattering) as a TOOL
  to access to . CORRELATION FUNCTI
  BEYOND THE 2nd ORDER

- NEAR EDGE STRUCTURE in HIGHLY CORRELATED SYSTEMS
  (Rare earths, high Tc's)
  as an electronic PROBE for
  VALENCY
  MAGNETISM

- HOW TO GO BEYOND THE ONE ELECTRON PICTURE .

- ------

THEREFORE ⟶ EXTRA WORK

X-ray Absorption Principles, Applications, Techniques of EXAFS, SEXAFS, XANES, ...
Ed. by J.C. Koningsberger, R. Prins, WILEY Interscience Pub.

A HISTORY OF X-RAY ABSORPTION FINE STRUCTURES

R. Stumm von Bordwehr
Laboratoire de Physique du Solide
Université de Nancy I
B.P. 239, F-54506 Vandoeuvre-lès-Nancy

Annales de Phys.
1989 / 14 / Aout
p 377-400

1. The discovery of X-ray absorption edges

1.1. The prehistory

The question of the origins is always involved, but it would be difficult to date back the X-ray absorption spectroscopy before the eighth of November 1895 in the evening.

That very day Wilhelm Conrad Röntgen was studying the discharge of electricity in rarefied gases by operating a Hittorf tube (some kind of Crookes tube) wrapped in a black cardboard. Some distance apart, there was a screen covered with barium platinum cyanide. Much to his surprise Röntgen saw the screen glowing: the first X-ray was detected. He reported his observations in a local journal (Röntgen 1895) where, almost incidentally, he named the new rays in a footnote: "Der Kürze halber möchte ich den Ausdruck "Strahlen" und zwar zur Unterscheidung von anderen den Namen "X-Strahlen" gebrauchen (to shorten I shall use the designation "rays", and to differentiate it from the others the naming "X rays")".

The news spread very fast over the world and created an extraordinary enthusiasm (rather comparable to the one caused by the high T_C supraconductors almost a century later): only in 1896 more than 1000 papers were published on the subject (Segrè 1980).

The study of the influence of X-rays on matter began immediately. In the course of experiments carried out in the laboratory of the Ecole Normale Supérieure, Jean Perrin (1897) noticed that the metals irradiated emitted charged particles. In 1898 Georges Sagnac discovered that "La surface d'un métal M, frappée par les rayons X, émet de nouveaux rayons que j'ai appelés *rayons secondaires du métal* M [... et qui ont] la propriété d'être absorbés complètement par le métal M qui les émet [?] (the surface of a metal M, receiving X-rays, emits new rays that I call secondary rays of the metal M and which have the property of being completely absorbed by the metal M which emits them)" (Sagnac 1898a). This was the first allusion to the fact that chemical elements could emit characteristic radiations. Three years later, Sagnac wrote a review article entitled "X-rays, matter and electricity", in which he came to the conclusion that: "Le pouvoir de transformation d'un métal vis-à-vis des rayons X [la fluorescence X] paraît distinguer ce métal d'un autre métal, sauf quand les poids atomiques sont assez voisins (Pb et Pt) ou que les métaux sont des éléments chimiques analogues (Fe et Ni). L'étude de l'action électrique d'un corps frappé par les rayons X permet d'y reconnaître la présence d'une petite quantité [illegible]

NOV 1895 Röntgen

97.35

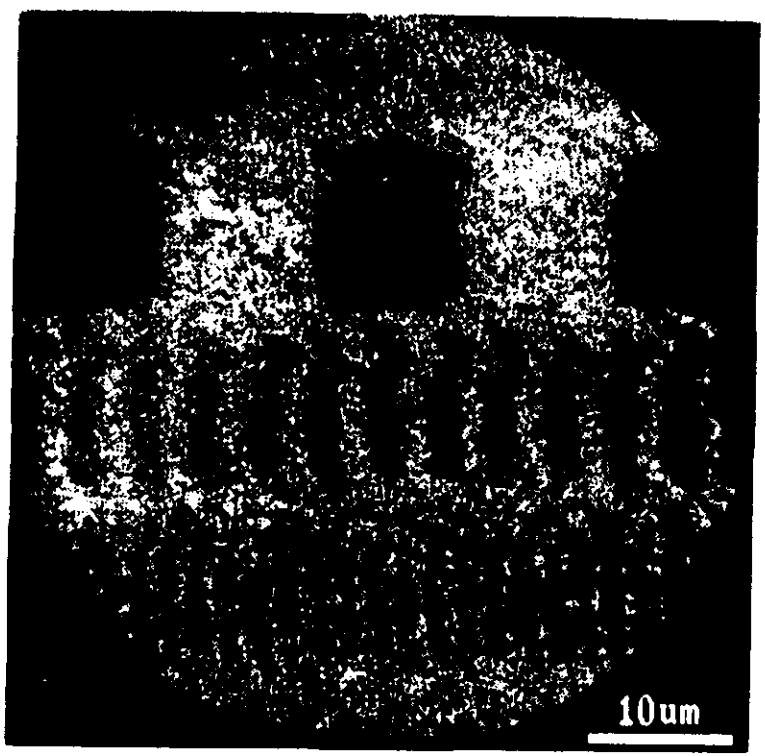

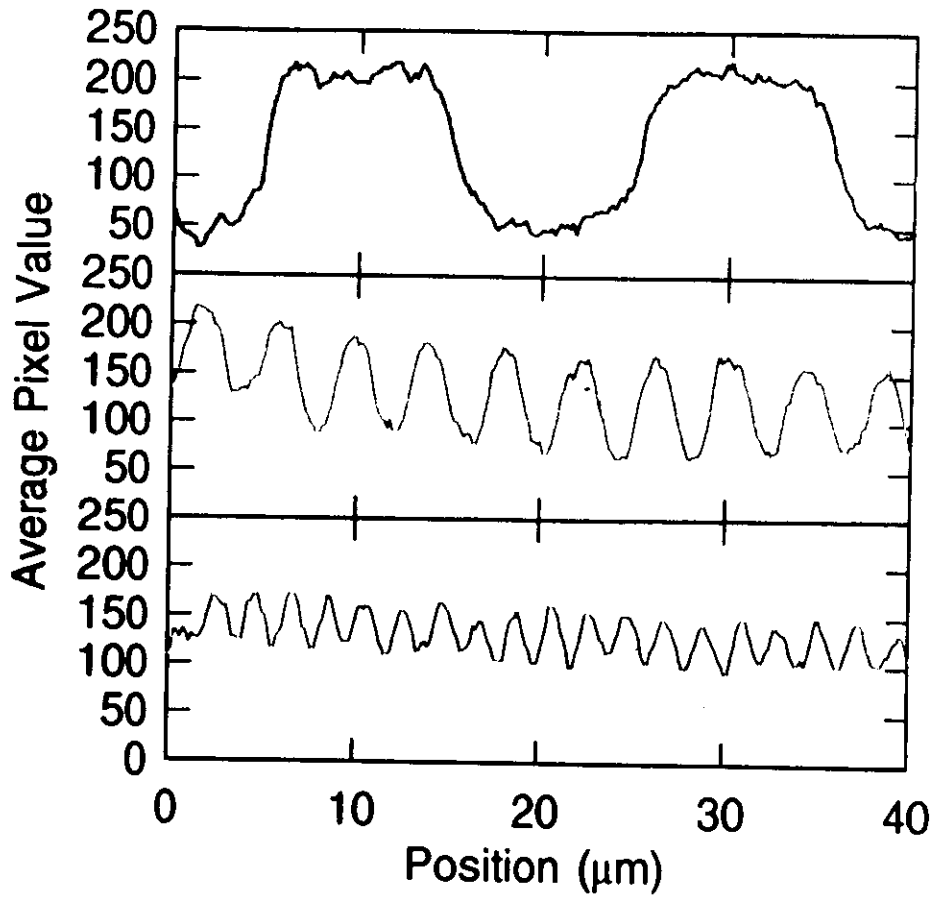

IMAGE =

LEFT HANDED $h\nu$

—

RIGHT HANDED $h\nu$

Co L_3 778 eV
(1.. 793 eV)

J. Stöhr, B. Tonner

MCXD Microscopy

Diff. Image @ 778eV L_{III} 793eV L_{II} 2μ → 3.1

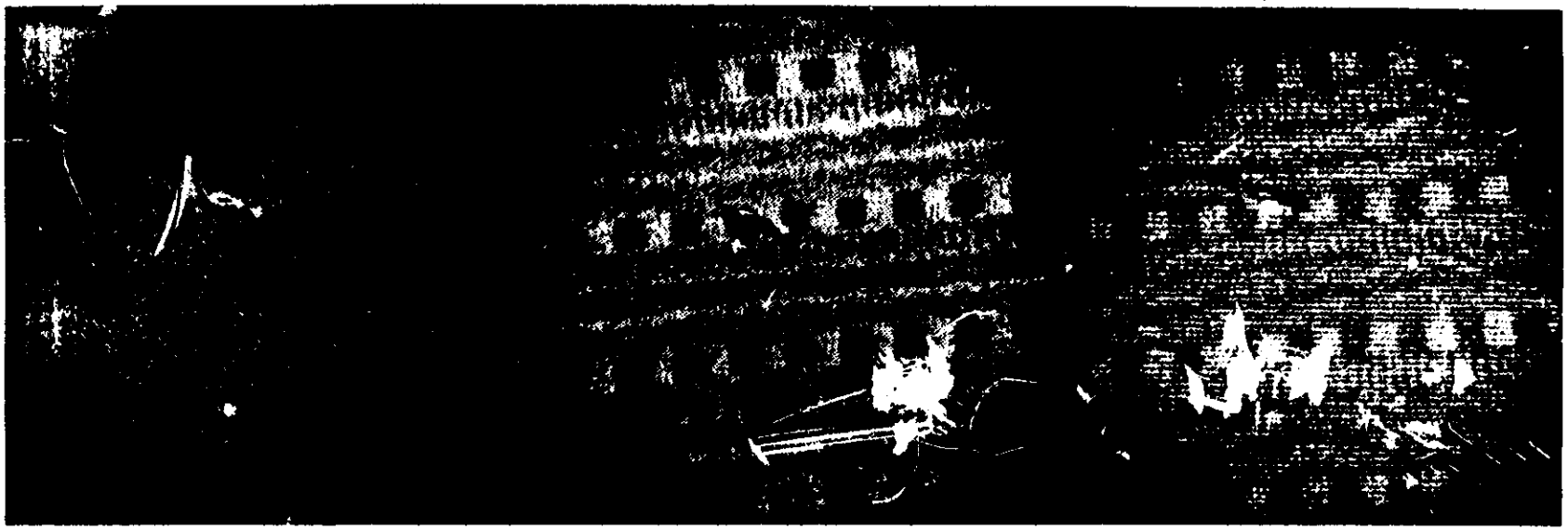

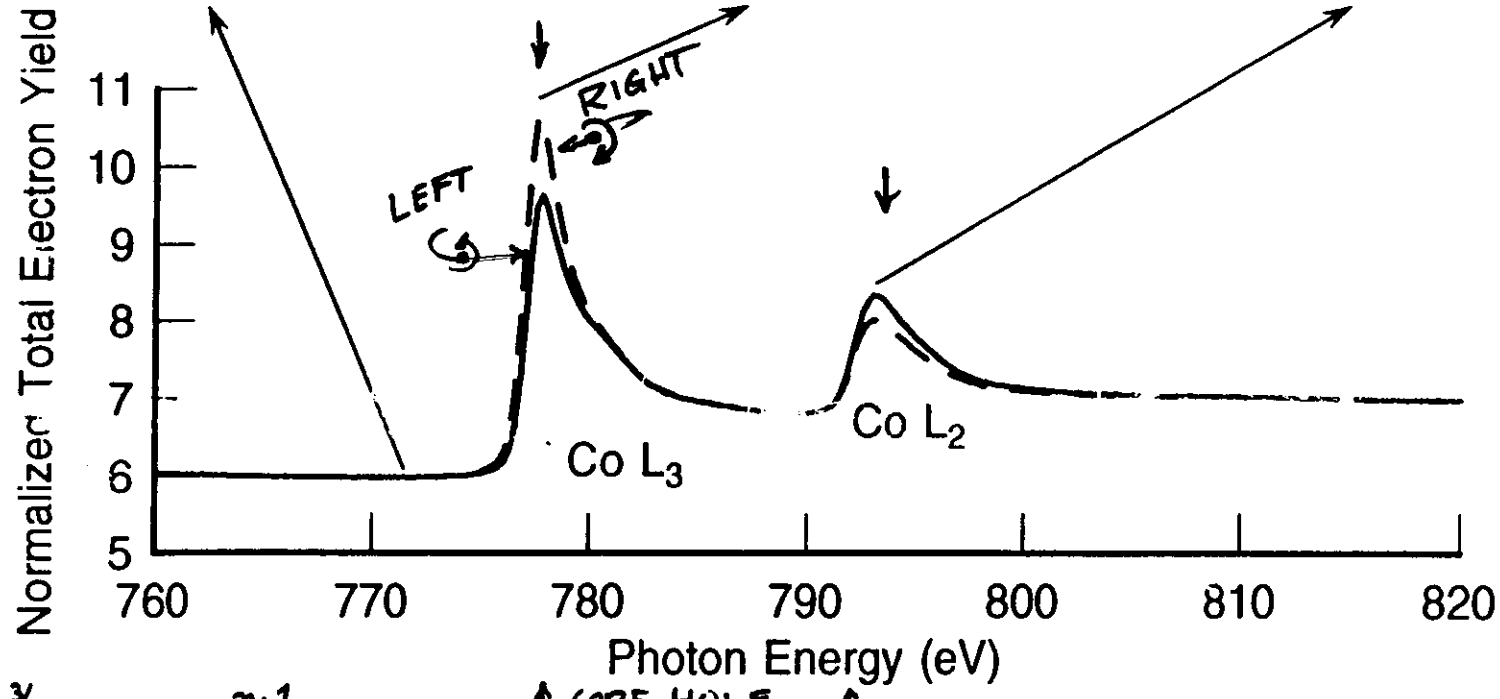

Fig. 2

J. STÖHR et al. (Nature) 93 Tb. Co from a disk mat.

$2p^{3/2}_{2p^{1/2}} \longrightarrow d^{n+1}$ $J=3/2$ ↑ CORE HOLE SPIN-ORBIT SPLIT ↑ $J=1/2$

YWu MCXD_ms

Stöhr et al. 1983

93-5

Microscopy of magnetic domains in ultra-thin films by x-ray dichroism

- D. Spanke, J. Dresselhaus, F.U. Hillebrecht, E. Kisker, University of Düsseldorf
- N.B. Brookes, J.B. Goedkoop, ESRF

Photo Emission Electron Microscope

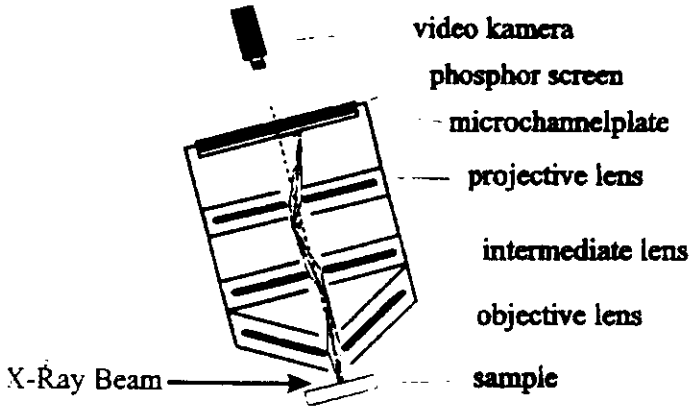

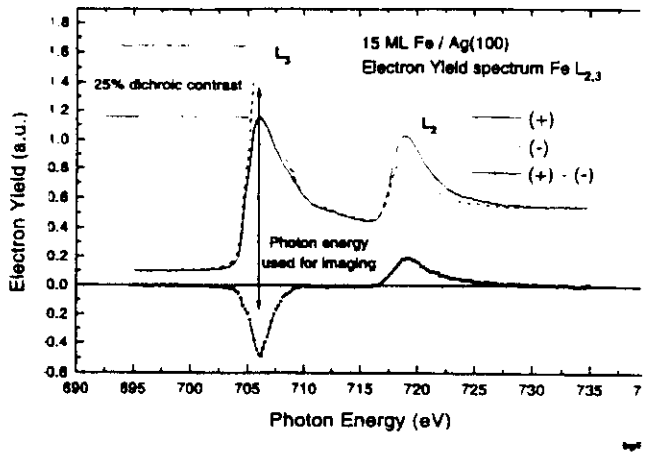

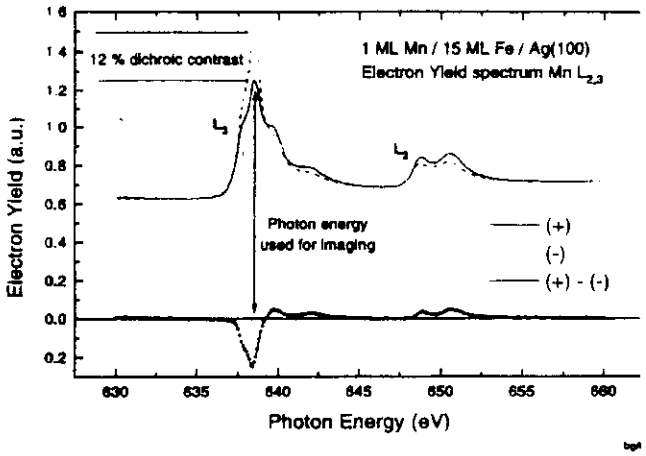

15 ML film of Fe on Ag (100)

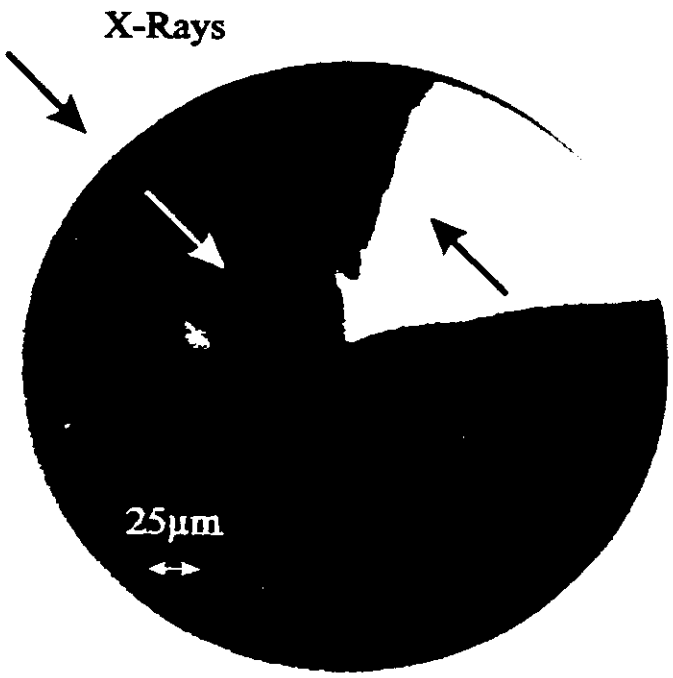

Three Domain directions
yellow: parallel to light helicity
blue: anti-parallel to light helicity
green: normal to light helicity

0.5 ML Mn on a 15 ML film of Fe on Ag (100)

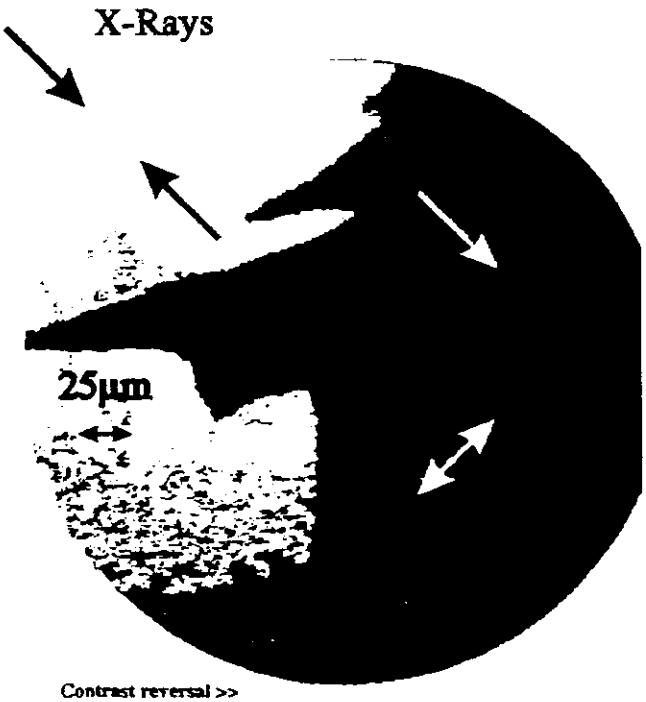

Contrast reversal >>
anti-ferromagnetic coupling of Mn with Fe substrate

Spectromicroscopy

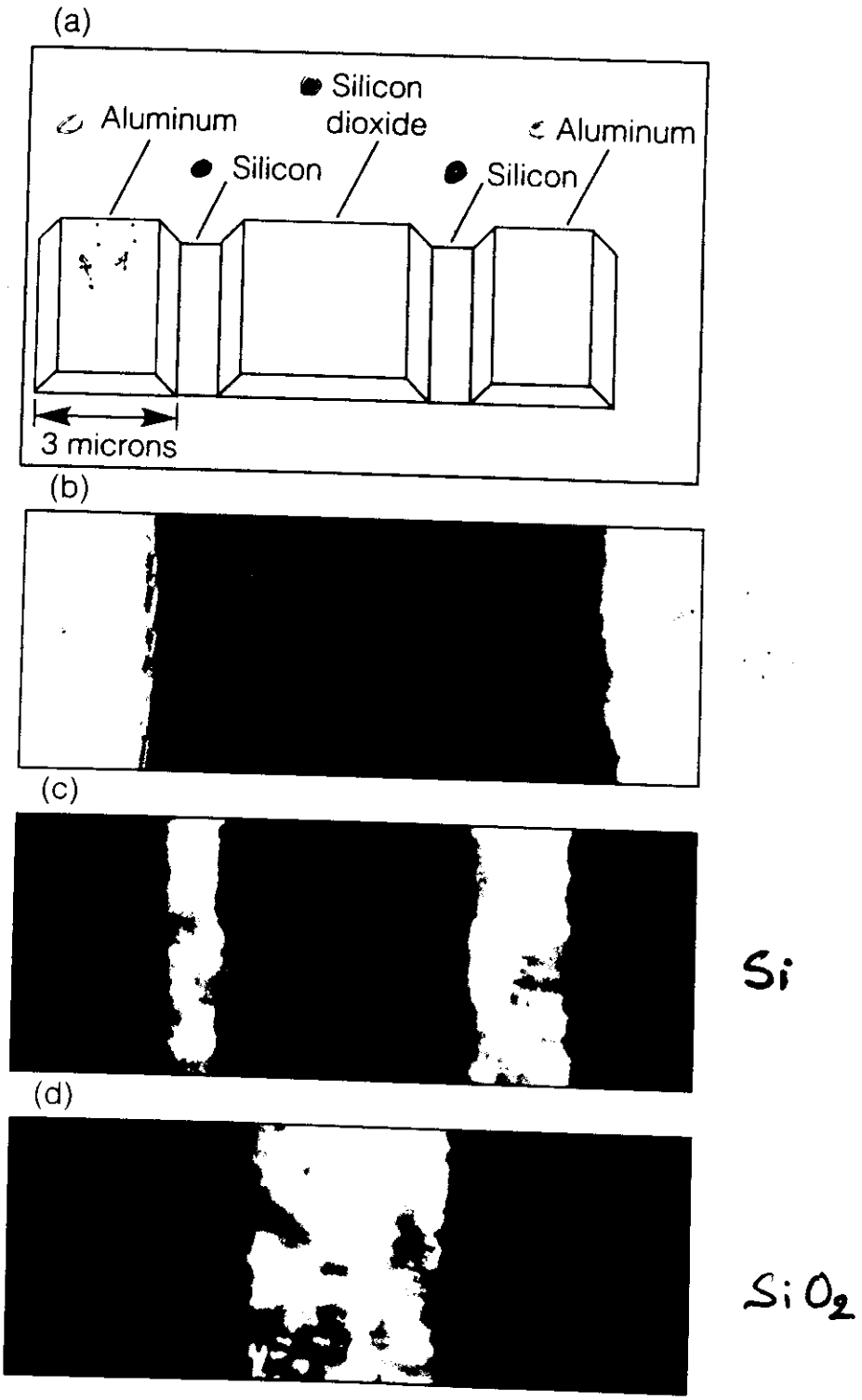

PHOTON SOURCES

energy tunable
polarisation tunable

(SR)

element selectivity
spin sensitivity
monolayer sensitivity
anisotropy sensitivity

valence sensitivity
local environment
probe

i.e structural
electronic
magnetic
information